

Rothamsted Repository Download

A - Papers appearing in refereed journals

Bianchetti, R. E., De Luca, B., De Haro, L. A., Rosado, D., Demarco, D., Conte, M., Bermudez, L, Freschi, L., Fernie, A. R., Michaelson, L. V., Haslam, R. P., Rossi, M. and Carrari, F. 2020. Phytochrome-dependent temperature perception modulates 2 isoprenoid metabolism. *Plant Physiology*. May, p. 00019.2020.

The publisher's version can be accessed at:

- <https://dx.doi.org/10.1104/pp.20.00019>

The output can be accessed at:

<https://repository.rothamsted.ac.uk/item/97q56/phytochrome-dependent-temperature-perception-modulates-2-isoprenoid-metabolism>.

© 1 May 2020, Please contact library@rothamsted.ac.uk for copyright queries.

1 **Short title:** PHYs temperature perception and plastid metabolism

2 **PHYTOCHROME-DEPENDENT TEMPERATURE PERCEPTION MODULATES**
3 **ISOPRENOID METABOLISM**

4 Ricardo Bianchetti^{1‡}, Belen De Luca^{2‡}, Luis A de Haro^{2†}, Daniele Rosado^{1††}, Diego
5 Demarco¹, Mariana Conte³, Luisa Bermudez^{3,4}, Luciano Freschi¹, Alisdair R. Fernie⁵,
6 Louise V Michaelson⁶, Richard P Haslam⁶, Magdalena Rossi^{1‡}, Fernando Carrari^{2,4†*}

7 ¹Departamento de Botânica, Instituto de Biociências, Universidade de São Paulo, São
8 Paulo, Brasil.

9 ²Instituto de Fisiología, Biología Molecular y Neurociencias (IFIBYNE-UBA-CONICET)
10 Ciudad Universitaria, C1428EHA Buenos Aires, Argentina.

11 ³Instituto de Agrobiotecnología y Biología Molecular (IABIMO), CICVyA - INTA;
12 CONICET, Argentina.

13 ⁴Cátedra de Genética, Facultad de Agronomía, Universidad de Buenos Aires, Buenos Aires,
14 Argentina.

15 ⁵Max Planck Institute of Molecular Plant Physiology, Wissenschaftspark Golm, Am
16 Mühlenberg 1, Potsdam-Golm, D-14476, Germany.

17 ⁶Department of Plant Sciences, Rothamsted Research, Harpenden, Herts, AL5 2JQ, UK.

18 †Current address: Department of Plant and Environmental Sciences, Weizmann Institute of
19 Science, Rehovot 76100, Israel

20 ††Current address: Cold Spring Harbor Laboratory, 1 Bungtown Road, Cold Spring Harbor,
21 New York 11724, USA

22 * Corresponding Author.

23 Fernando Carrari

24 Phone: +54 11 4576-3386 / 3368 ext 238

25 email: fcarrari@fbmc.fcen.uba.ar

26 ‡ These authors contributed equally to this work.

27

28 **One-sentence summary:** Phytochrome-mediated temperature perception compromises
29 plastidial development and function, impairing isoprenoid metabolism in tomato leaves and
30 fruits.

31

32 **Author contributions**

33 RB performed most of the experiments and analyzed the data; BDL and LAH performed
34 experiments and analyzed data; DR, DD and LB performed experiments; MC, LF, ARF,
35 LVM and RPH contributed to experimental design and provided technical assistance; RB,
36 MR, ARF and FC conceived the project, designed experiments and wrote the paper which
37 was revised and approved by all authors. FC agrees to serve as the author responsible for
38 contact and ensures communication.

39 **FUNDING**

40 This work was supported by FAPESP (Fundação de Amparo à Pesquisa do Estado de São
41 Paulo, Grant Number #2016/01128-9); CNPq (Conselho Nacional de Desenvolvimento
42 Científico e Tecnológico, Grant Number 440976/2016-2); European Union Horizon 2020
43 Research and Innovation Programme (Grant Agreement Number 679796), and ANPCyT
44 Agencia Nacional de Promoción Científica y Tecnológica, Argentina, Grant Number 2014-
45 0984 to F.C.). R.P.H and L.V.M. were supported by the BBSRC (Biotechnology and
46 Biological Sciences Research Council, UK) through the Tailoring Plant Metabolism
47 Institute Strategic Grant (BBS/E/C/000I0420) supporting R.P.H and the UK-Brazil
48 Alliance for Sustainable Agriculture scheme (BBS/OS/NW/000001). R.B. and D.R. were
49 recipient of FAPESP fellowships (#2017/24354-7 and #2015/14658-3). B.D.L and L.A.de
50 H. are CONICET fellows. L.B. and F.C are members of CONICET. M.R. was a recipient
51 of CNPq fellowship.

52

53 **Abstract**

54 Changes in environmental temperature influence many aspects of plant metabolism;
55 however, the underlying regulatory mechanisms remain poorly understood. In addition to
56 their role in light perception, phytochromes (PHYs) have been recently recognized as
57 temperature sensors affecting plant growth. In particular, in *Arabidopsis thaliana*, high
58 temperature reversibly inactivates PHYB, reducing photomorphogenesis-dependent
59 responses. Here, we show the role of phytochrome-dependent temperature perception in
60 modulating the accumulation of isoprenoid-derived compounds in tomato (*Solanum*
61 *lycopersicum*) leaves and fruits. The growth of tomato plants under contrasting temperature
62 regimes revealed that high temperatures resulted in co-ordinated up-regulation of
63 chlorophyll catabolic genes, impairment of chloroplast biogenesis, and reduction of
64 carotenoid synthesis in leaves in a PHYB1B2-dependent manner. Furthermore, by
65 assessing a triple *phyAB1B2* mutant and fruit-specific *PHYA*- or *PHYB2*-silenced plants, we
66 demonstrated that biosynthesis of the major tomato fruit carotenoid, lycopene, is sensitive
67 to fruit-localized PHY-dependent temperature perception. The collected data provide
68 compelling evidence concerning the impact of PHY-mediated temperature perception on
69 plastid metabolism in both leaves and fruit, specifically on the accumulation of isoprenoid-
70 derived compounds.

71 **Keywords:** carotenoid, chlorophyll, chloroplast, fleshy fruit, isoprenoids, phytochrome,
72 temperature, tomato.

73

74 INTRODUCTION

75 Temperature cues regulate plant primary and secondary metabolism, affecting several
76 agronomically important traits in crop species (Suwa et al., 2010; Bitá and Gerats, 2013;
77 Zhao et al., 2017). It has been established that heat disrupts chloroplast integrity leading to
78 further deficiencies of plastid-associated metabolites and a subsequent decline in plant
79 performance (Yamori and von Caemmerer, 2009; Spicher et al., 2017). The ability to
80 perceive stress conditions allows plants to adapt their metabolism in order to minimize any
81 harmful effects on fitness (Saidi et al., 2011).

82 PHYTOCHROMES (PHYs) have been extensively described as light receptors. The
83 biologically inactive PHY form (Pr) remains in the cytosol; however, once activated by red
84 light, the active form (Pfr) is translocated towards the nucleus where it assembles into
85 photobodies and triggers photomorphogenesis-associated responses (Rockwell et al., 2006).
86 The conversion of Pr to Pfr can be reversed by far-red light or darkness (Burgie and
87 Vierstra, 2014). PHYTOCHROME B (PHYB) has been associated with a quantitative trait
88 loci interval for thermoresponsive growth in *Arabidopsis thaliana* (Box et al., 2015). High
89 temperature reduces the abundance of Pfr by a quick and spontaneous reversion to Pr in a
90 light-independent manner, consequently decreasing the size of nuclear bodies in a process
91 termed thermoreversion (Legris et al., 2016). By contrast, lack of thermoreversion was
92 detected in the hyperactive *phyB* mutant resulting in the constitutive presence of
93 photobodies regardless of temperature condition (Huang et al., 2019). As such, the *A.*
94 *thaliana phyB* null mutant mimics the transcriptional profile and physiological parameters
95 of the wild-type counterpart grown under high temperature (Jung et al., 2016).

96 In tomato (*Solanum lycopersicum*) PHYs belong to a multigenic family encompassing five
97 members: PHYA, PHYB1, PHYB2, PHYE, and PHYF (Alba et al., 2000b). We have
98 previously demonstrated that PHYA, PHYB1, and PHYB2 positively control the
99 biosynthesis of isoprenoid-derived compounds in tomato fruits in response to light
100 (Bianchetti et al., 2018; Gramegna et al., 2018). PHYs post-translationally downregulate a
101 group of helix-loop-helix proteins named PHYTOCHROME INTERACTING FACTORS
102 (PIFs) (Park et al., 2018). PIFs derive from a multigenic family and have undergone sub-
103 and neofunctionalization at the mRNA level (Rosado et al., 2016). It has been shown that
104 SIPIF1a, SIPIF3, and SIPIF4 regulate carotenogenesis (Llorente et al., 2016), tocopherol

105 biosynthesis (Gramegna et al., 2018), and sugar metabolism (Rosado et al., 2019),
106 respectively, by (a) light-dependant mechanism(s).
107 Here, by analyzing the metabolic and transcriptional profile of wild-type and *phy*-mutant
108 tomato plants grown under contrasting temperature conditions, we showed that high
109 temperature results in the reduction of leaf chlorophyll (Chl) and carotenoid levels in a
110 PHYB1/B2-mediated manner through the regulation of Chl degradation and carotenoid
111 biosynthetic genes, respectively. Furthermore, our data also demonstrate that high
112 temperature or PHYAB1B2 impairment leads to the transcriptional downregulation of
113 carotenoid biosynthetic genes in fruits, resulting in reduced levels of lycopene. Data
114 obtained from fruit-specific *PHYA*- and *PHYB2*-silenced plants corroborated the role of
115 fruit-localized PHYs in carotenoid accumulation through an intricate network in which
116 master ripening transcription factors participate as mediators of temperature perception in
117 tomato fruits.
118
119

120 RESULTS

121

122 High temperature affects plants growth phenotype in tomato

123 To investigate the role played by PHYs in response to high temperature, 20-day-old plants
124 from wild type cv. MoneyMaker (MM), *phyB1* and *phyB2* single mutants, and the *phyB1B2*
125 double mutant were transferred to ambient-temperature (AT, 24°C/18°C) and high-
126 temperature (HT, 30°C/24°C) growing conditions (Supplemental Figure S1). Thirty days
127 post-transfer, *phy* mutants displayed more elongated internodes than MM adult plants, as
128 previously described (Kerckhoffs et al., 1997; 1997) under both temperature regimes,
129 indicating that this is a genotype-dependent phenotype. On the other hand, for all the
130 genotypes, HT promoted a narrower stem diameter, reduced leaf area, and less branching
131 (Figure 1A), exposing a HT-dependent phenotype. Thus, in these plants, no PHY-
132 dependent HT phenotype was observed, which contrasted with that described in *A. thaliana*
133 seedlings, where HT increases elongation in a PHY-mediated manner (Jung et al., 2016).
134 Moreover, no differences in relative water contents in leaves and fruits were observed
135 between either genotypes or treatments (Supplemental Figure S2). These results indicate
136 that the applied temperature treatments affected plant growth without changing the water
137 status of the plants, rendering the experimental setup suitable to study the impact of
138 temperature on tomato metabolism in a PHY-dependent manner.

139

140 High temperature alters chlorophyll metabolism and fluorescence parameters in a 141 PHYB1/B2-dependent manner

142 Evidences about the role of PHYB on Chl biosynthesis (Inagaki et al., 2015) and its
143 function as a thermosensor in *A. thaliana* (Jung et al., 2016; Legris et al., 2017) led us to
144 investigate the effects of PHYB1/B2-dependent temperature perception on tomato Chl
145 metabolism. To address this question, Chl levels and fluorescence parameters were
146 analyzed in leaves from 85-day-old plants of *phyB1*, *phyB2*, and *phyB1B2* mutants
147 alongside the corresponding wild-type genotype. Notably, HT resulted in a significant
148 reduction of total leaf Chl content in MM genotype. However, the mutants were virtually
149 insensitive to this temperature effect. Interestingly, regardless of the temperature treatment,
150 leaf Chl content in the *phyB1B2* double mutant was the same as that observed in MM under

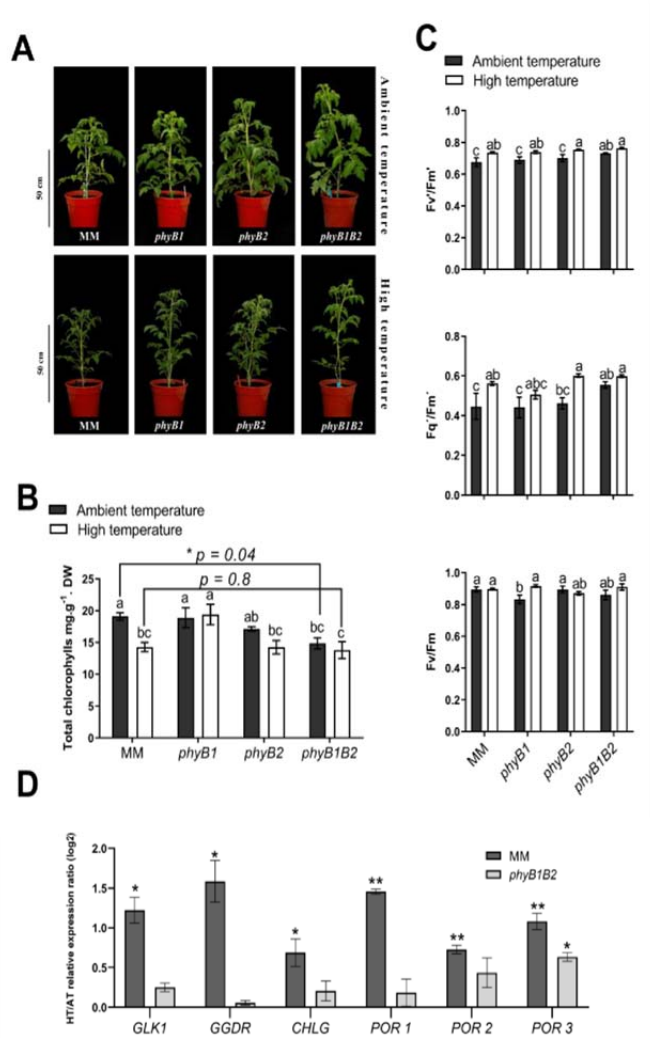


Fig. 1. PHYB1/B2 are involved in temperature perception impacting leaf chlorophyll metabolism and fluorescence parameters in tomato. (A) Side view of 50-day-old *S. lycopersicum* cv. Moneymaker (MM) plants and *phyB1*, *phyB2* and *phyB1B2* knockout mutants grown under ambient (AT, day/night 24 °C/18 °C) and high-temperature (HT, day/night 30 °C/24 °C). (B) Quantification of total chlorophylls in the seventh fully expanded leaf from 85-days-old plants. Each bar represents mean \pm SE (C) PSII maximum efficiency (F_v/F_m'), PSII operating efficiency (F_q'/F_m') and maximum quantum efficiency of PSII (F_v/F_m) measured in the sixth fully expanded leaf from 85-days-old plants. $n =$ at least five biological replicates. Each bar represents mean \pm SE. Different letters indicate statistically significant differences according to Fisher's multiple comparison test ($p < 0.05$). Asterisks (* $p < 0.05$, ** $p < 0.01$) indicate statistically significant differences by two-tailed Student *t* test between MM and *phyB1B2* in the same environmental condition. (D) HT/AT relative expression ratio of *GLK1*, *GGDR*, *CHLG*, *POR1*, *POR2* and *POR3* mRNA abundance in MM and *phyB1B2* mutant leaf samples from 85-days-old plants. $n =$ at least three biological replicates. Each bar represents mean \pm SE. Asterisks (* $p < 0.05$, ** $p < 0.01$) indicate statistically significant differences by two-tailed Student *t* test between AT and HT within the same genotype. Genes are denoted according to the abbreviations: *GLK1*, GOLDEN2-LIKE1; *GGDR*, GERANYLGERANYL DIPHOSPHATE REDUCTASE; *CHLG*, CHLOROPHYLL SYNTHASE; *POR*, PROTOCHLOROPHYLLIDE OXIDOREDUCTASE.

151 HT (Figure 1B). Additionally, under both temperature conditions, the *phyB1B2* double

152 mutant, but not the *phyB1* or *phyB2* single mutants, exhibited values of light-adapted PSII
153 maximum efficiency (F_v'/F_m') and PSII operating levels (F_q'/F_m') similar to those
154 observed in MM under HT conditions and higher than MM under AT conditions. No
155 impact of HT on dark-adapted PSII maximum quantum efficiency (F_v/F_m) was observed in
156 any genotype (Figure 1C).

157 In order to gain insights into the regulatory role of PHYB1/B2 as temperature mediators in
158 Chl metabolism, we further investigated the mRNA levels of genes encoding key proteins
159 involved in Chl biosynthesis that previously showed PHY-dependent transcriptional
160 regulation (Gramegna et al., 2018; Alves et al., 2020). These genes included
161 *GERANYLGERANYL DIPHOSPHATE REDUCTASE (GGDR)*, the last enzyme for phytyl
162 diphosphate (PDP) chain synthesis (Almeida et al., 2015); the tetrapyrrole biosynthetic
163 gene *PROTOCHLOROPHYLLIDE OXIDOREDUCTASE (POR)*; three *loci* exist in the
164 tomato genome named *POR1* (Solyc12g013710), *POR2* (Solyc10g006900) and *POR3*
165 (Solyc07g054210), as revealed by the phylogenetic analyses presented in Supplemental
166 Figure S3); and *CHLOROPHYLL SYNTHASE (CHLG)*, which condensates the tetrapyrrole
167 ring with the PDP (Almeida et al., 2015). Additionally, as a marker of chloroplast
168 biogenesis and activity, we also included in the analysis the master transcriptional factor
169 *GOLDEN2-LIKE1 (GLK1)* (Nguyen et al., 2014), which regulates the expression of Chl
170 biosynthetic genes (Nakamura et al., 2009). HT resulted in significant increases in *GLK1*,
171 *GGDR*, *CHLG*, *POR1*, *POR2*, and *POR3* mRNA levels in the leaves of MM genotype,
172 whereas *phyB1B2* double mutant displayed a constitutive HT phenotype regarding
173 expression of Chl biosynthetic genes (except for the case of *POR3*, Figure 1D,
174 Supplemental Table S1), exposing a PHYB1/B2-dependent induction of Chl biosynthesis
175 under HT conditions.

176 Taken together, these results show that Chl accumulation is regulated by temperature in a
177 PHYB1/B2-dependent manner synergistically, and reveal that temperature-induced Chl
178 reduction is not the consequence of PHY-mediated impairment in Chl biosynthesis.

179

180 **High temperature and PHYB1/B2 deficiency impact chloroplast biogenesis and**
181 **differentiation**

182 The effect of PHYs (Oh and Montgomery, 2014; Martin et al., 2016) and temperature
183 (Takahashi and Murata, 2008; Van Eerden, et al., 2015) on chloroplast biogenesis and
184 structure have already been studied separately in several plant species. However, these two
185 variables have not been previously assayed in an integrated manner in tomato, nor have
186 they been assessed in any other crop species where chloroplasts determine nutritional
187 quality. Here, we evaluated whether the HT-induced impact on chloroplast development is
188 mediated by PHYB1/B2 in tomato. Similarly to that observed for 85-day-old plants (Figure
189 1B), 21-day-old plants of MM, grown under HT conditions, and the *phyB1B2* mutant,
190 regardless of the temperature condition, showed chlorotic symptoms (red arrows Figure
191 2A). This visual phenotypic difference agreed with lower measurements of leaf Chl content
192 (Figure 2B), strengthening the idea of PHYB1/B2 as a mediator of temperature perception
193 modulating leaf Chl metabolism. Thus, to address whether differences in Chl levels were
194 associated with changes in chloroplast biology, plastid quantification and ultrastructure
195 analyses were performed in mesophyll cells. Microscopy data revealed a reduction in the
196 number of chloroplasts per mesophyll cell in MM plants grown under HT and in the
197 *phyB1B2* double mutant cells under AT and HT compared to MM genotype under AT
198 (Figure 2C). Interestingly, the *phyB1B2* double mutant still showed a slight temperature
199 response, indicating the existence of PHY-independent temperature sensing, as reported in
200 *A. thaliana* (Fujii et al., 2017; Ma et al., 2016). Additionally, leaves developed under HT
201 exhibited remarkable changes in chloroplasts ultrastructure (Figure 2D). Chloroplasts of
202 MM developed under HT and those of the *phyB1B2* double mutant, under both temperature
203 regimes, showed reduced grana stacking and dilated thylakoid lumen in comparison to MM
204 under AT.

205 PIF transcription factors have shown to mediate PHY-dependent temperature perception
206 and, in particular PIF1 and PIF3, have been shown to regulate chloroplast development in
207 *A. thaliana* (Kim et al., 2016, Stephenson et al., 2009). In tomato PIF4 has been shown to
208 participate in temperature-dependent seedling elongation (Rosado et al., 2019). Although
209 PIFs accumulation is mostly regulated post-translationally, we found that *PIF1b* mRNA
210 levels increase under HT in the MM genotype but the *phyB1B2* double mutant was
211 insensitive (Supplemental Figure S4A). We also identified significant upregulation of *PIF3*
212 mRNA in response to HT in MM and in the *phyB1B2* mutant regardless of temperature.

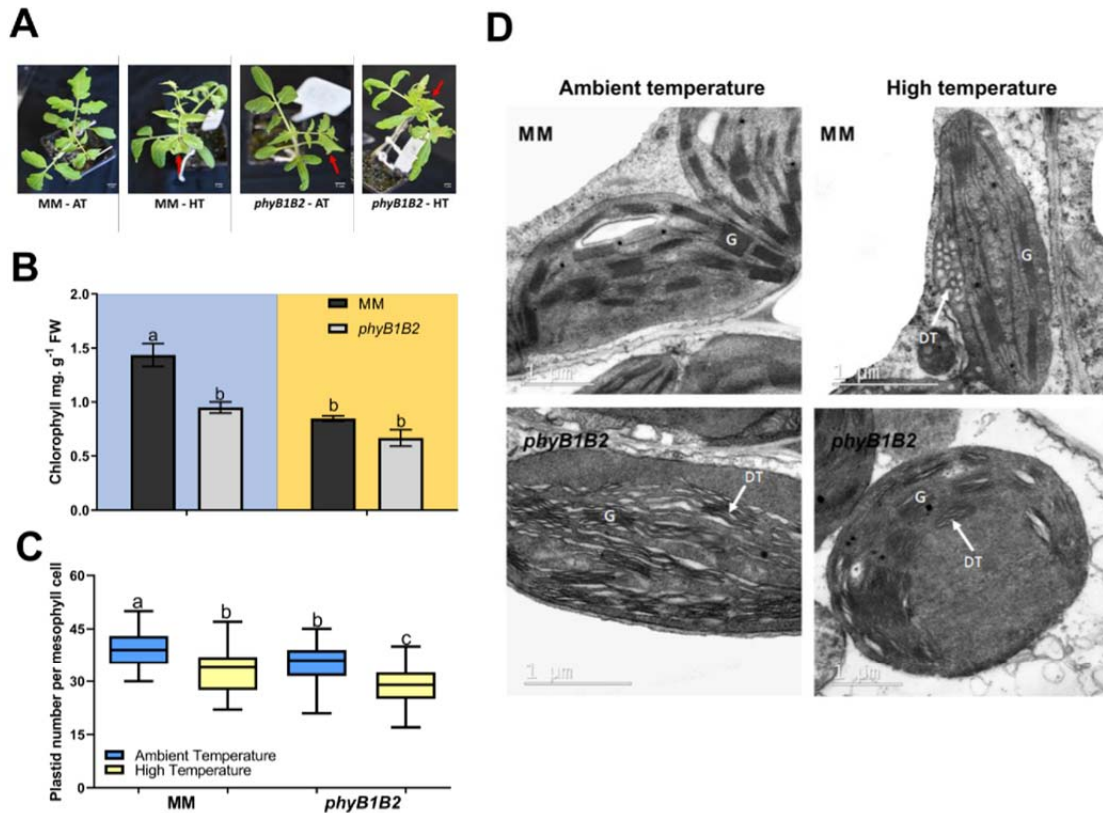


Figure 2. High temperature affects plastid biogenesis and development in leaves in a PHYB1/2-dependent manner. (A) Visualization of a representative leaf of 21-day-old *S. lycopersicum* cv. Moneymaker (MM) and *phyB1B2* knockout mutants after two weeks under ambient (AT, day/night 24 °C/18 °C) and high-temperature (HT, 30 °C/24 °C). Red arrows indicate chlorotic leaves (MM at HT, *phyB1B2* at AT and *phyB1B2* at HT). (B) Quantification of total chlorophylls in leaves cultivated under AT (blue background) and HT (yellow background). n = at least three biological replicates. Each bar represents mean ± SE. (C) Plastid density per mesophyll cell. Values represent chloroplast quantification of ± 70 cells. Different letters indicate statistically significant differences according to Fisher's multiple comparison test ($p < 0.05$). Each bar represents mean ± SE. (D) Representative TEM images of chloroplast from MM and *phyB1B2* leaves grown under AT and HT. G indicates grana and DT indicated dilated thylakoids.

213 These alterations in *PIF1b* and *PIF3* mRNA levels may explain, at least in part, the reduced
 214 number of plastids and their altered ultrastructure.

215 In conclusion, our data suggest that temperature perception mediated by PHYB1/2 has an
 216 impact on chloroplast development that ultimately determines their structure and function.

217

218 **PHYB1/B2 inactivation mediated by high temperature enhances chlorophyll**
219 **degradation pathway in leaves**

220 In *A. thaliana*, PHYB regulates leaf senescence in response to light conditions through
221 PIF4/PIF5, which in turn induce Chl breakdown (Sakuraba et al., 2014). However, it is
222 unknown how PHYB-mediated temperature perception operates on Chl catabolism. The
223 Chl degradation pathway operates in tomato leaves during senescence (Lira et al., 2014;
224 Guyer et al., 2014), leading to phytol chain removal followed by the linearization of the
225 tetrapyrrole ring involving several enzymatic steps (Hörtensteiner, 2013; summarized in
226 Figure 3A). In brief, Chl *a* is converted to an intermediate phytol-free chlorophyllide *a*
227 (Chlide *a*) or a magnesium-free pheophytin *a* (Pheo *a*) form by CHLOROPHYLLASE
228 (CLH) and STAY GREEN (SGR), respectively. Chlide *a* and Pheo *a* are subsequently
229 converted into pheophorbide *a* (Pheide *a*) through dechelation, mediated by STAY
230 GREEN-LIKE (SGR-like), and dephytylation, mediated by PHEOPHYTINASE (PPH),
231 respectively. Finally, Pheide *a* is linearized by PHEOPHORBIDE A OXYGENASE (PAO)
232 to yield a red chlorophyll catabolite (RCC). To understand Chl reductions observed under
233 HT and in the *phyB1B2* mutant, we therefore measured the mRNA levels of *CLH1*, *CLH2*,
234 *CLH4*, *SGR*, *PPH*, *SGR-like*, and *PAO*.

235 mRNA levels of *CLH2*, *CLH4*, *PPH*, *SGR-like*, and *PAO* were at least two-fold up-
236 regulated in MM plants cultivated under HT (Figure 3B). Consistent with our proposed role
237 of PHYB1/B2 in temperature perception, regardless of the temperature condition, the
238 *phyB1B2* double mutant showed mRNA levels similar to those observed in MM under HT
239 for the *CLH4*, *PPH*, *SGR-like*, and *PAO* genes (Figure 3A and Figure 3B). It has been
240 reported that Chl degradation is triggered by dark-induced senescence and mediated by
241 PHY perception and PIF signaling (Sakuraba et al., 2014). In particular, SGR and PAO
242 enzyme-encoding genes are directly upregulated by PIF4 and PIF5 in *A. thaliana* (Song et
243 al., 2014; Zhang et al., 2015). Even though the *PIF4* mRNA profile did not respond to
244 temperature in our experiment (Supplemental Figure S4A), we cannot formally rule out its
245 involvement in the regulation of this process, considering that we were able to identify PIF-
246 binding motifs in the four genes that showed PHYB1/B2-mediated temperature modulation,
247 specifically *CLH4*, *PPH*, *SGR-like*, and *PAO* (Supplemental Figure S4B). This observation
248 suggests that the PHY-PIF module acts similarly in tomato as in *A. thaliana*.

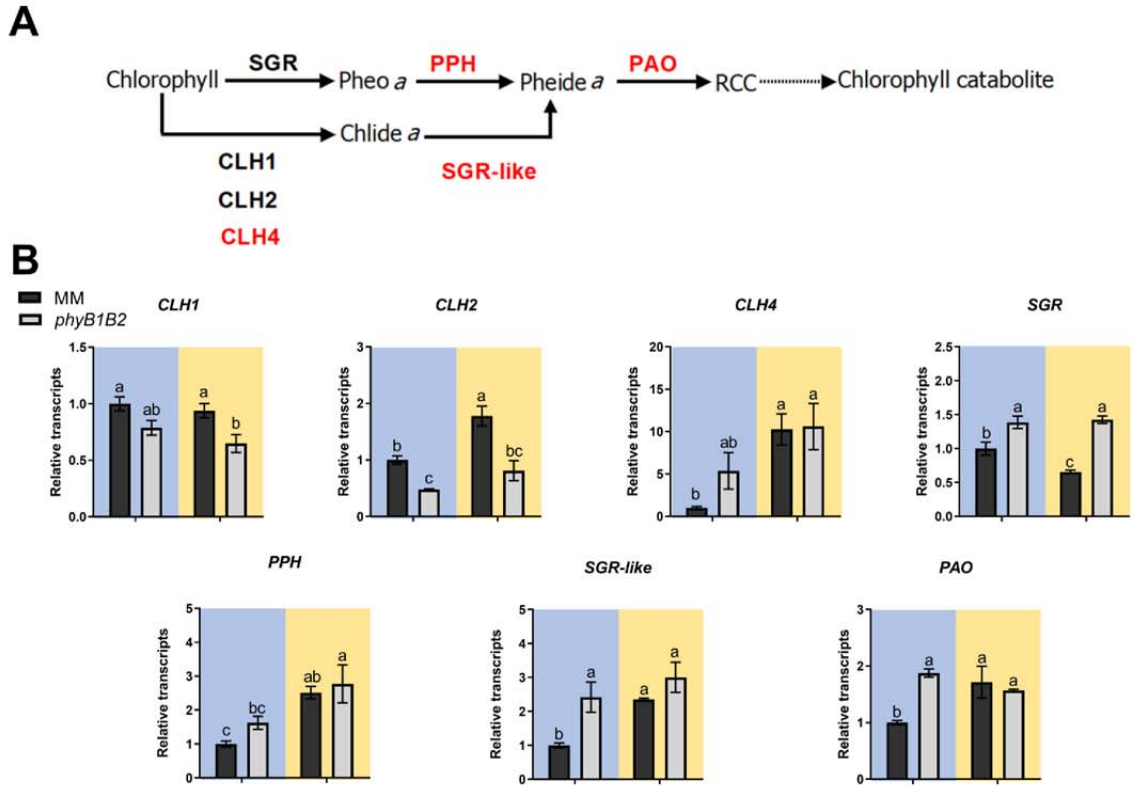


Figure 3. High temperature enhances chlorophyll degradation in leaves in a PHYB1/B2-dependent manner.

(A) Schematic model of chlorophyll degradation pathway. Enzymes and metabolites are denoted according to the following abbreviations: Pheo *a*, pheophytin *a*; Chlide *a*, chlorophyllide *a*; Pheide *a*, pheophorbide *a*; RCC, red chlorophyll catabolite; CLH, CHLOROPHYLLASE; SGR, STAY GREEN; SGR-like, PPH, PHEOPHYTINASE; STAY GREEN-LIKE; PAO, PHEOPHORBIIDE *a* OXYGENASE. The enzymes highlighted in red are those that showed to be regulated by temperature in a PHYB1/B2-dependent manner according to Figure 3B. (B) Relative mRNA levels of chlorophyll degrading enzymes encoding genes in Moneymaker (MM) and *phyB1B2* mutant leaf samples from 85-day-old plants grown under ambient temperature (AT, 24 °C/18 °C - blue background) and high-temperature (HT, 30 °C/24 °C - yellow background). Expression levels are relative to MM – AT condition. n = at least three biological replicates. Each bar represents mean \pm SE. Different letters indicate statistically significant differences according to Fisher's multiple comparison test ($p < 0.05$).

249 Collectively, these results demonstrated that PHYB1/B2 represses Chl catabolism genes in
 250 a temperature-dependent manner in tomato leaves.

251

252 **PHYB1/B2-dependent temperature perception regulates leaf carotenoid biosynthesis**
 253 **at the transcriptional level**

254 Alongside the induction of the Chl degradation pathway, the HT treatment and the
255 *phyB1B2* double mutation resulted in over 30% reduction of total leaf carotenoids (Figure
256 4A). To understand the molecular basis of this reduction, we analyzed the transcriptional
257 profile of carotenoid biosynthetic enzyme-encoding genes. *GERANYLGERANYL*
258 *DIPHOSPHATE SYNTHASE 1* (*GGPS1*), which produces the carotenoids precursor
259 geranylgeranyl diphosphate (Quadrana et al., 2013), was shown to be downregulated both
260 in response to HT and in the *phyB1B2* double mutant (Figure 4B). By contrast, genes
261 encoding carotenoid downstream enzymes, such as PHYTOENE SYNTHASE 2 (*PSY2*),
262 PHYTOENE DESATURASE (*PDS*), CHROMOPLAST-SPECIFIC LYCOPENE β
263 CYCLASE (*CYC β*), and CHLOROPLAST-SPECIFIC LYCOPENE β CYCLASE (*LYC β*),
264 did not show *PHYB1/B2*-mediated temperature modulation (Supplemental Figure S5).
265 Thus, the results presented above indicate that, in tomato leaves, the accumulation of
266 chloroplast photosynthetic pigments is controlled through transcriptional adjustments of
267 Chl degradation and carotenoid biosynthesis genes by the ambient temperature in a
268 *PHYB1/B2*-dependent manner.

269

270 **Fruit carotenoid contents are modulated by temperature through *PHYA* and** 271 ***PHYB1/B2***

272 A role for *PHYs* in tomato fruit carotenoid accumulation has long been proposed (Alba et
273 al., 2000a; Gupta et al., 2014), and we recently demonstrated that fruit-localized *PHYA* and
274 *PHYB2* positively influence fruit carotenoid accumulation (Bianchetti et al., 2018). Aiming
275 to evaluate the temperature effects on carotenogenesis, we followed two complementary
276 approaches: i) investigate the single *phyA*, *phyB1*, and *phyB2* mutants and the triple
277 *phyAB1B2* mutant and ii) analyze fruit-specific RNAi *PHYA*- and *PHYB*-silenced lines in
278 the Micro-Tom (MT) background (*PHYA^{RNAi}* and *PHYB2^{RNAi}*). This would allow us to
279 unravel whether fruit-localized *PHYs* regulate carotenogenesis in a temperature-dependent
280 manner in this organ and if this mechanism is genotype-independent.

281 Except for the *phyAB1B2* triple mutant, ripe fruits harvested from HT-grown plants
282 exhibited reductions in total carotenoid content compared to that in AT counterparts (Figure
283 5A). Ripe fruits collected from single *phyA*-, *phyB1*-, and *phyB*-mutant plants or double
284 *phyB1B2*-mutant plants grown under AT displayed lower total carotenoid levels those that

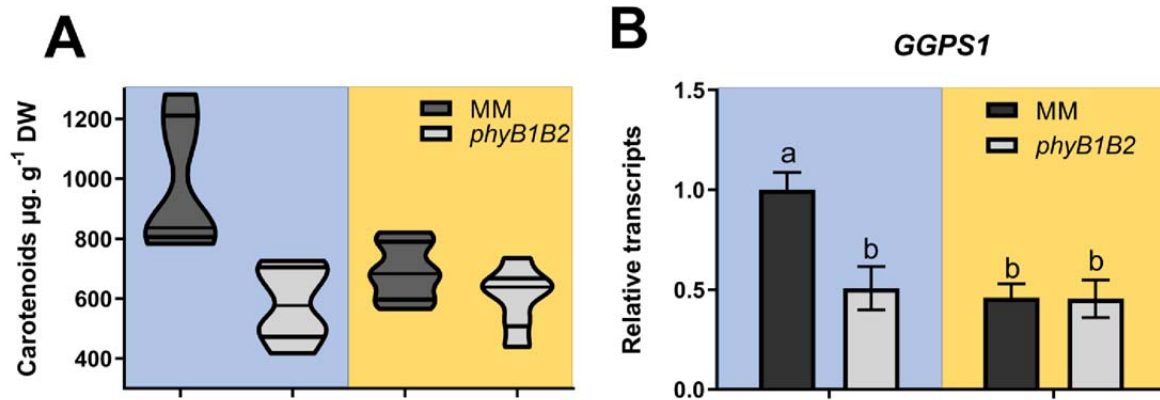


Figure 4. PHYB1/B2-dependent temperature perception transcriptionally regulates leaf carotenogenesis.

(A) Total carotenoid levels expressed in μg per g of dry weight. $n =$ at least five biological replicates. (B) Relative mRNA levels of *GGPS1* gene in Moneymaker (MM) and *phyB1B2* mutant leaf samples from 85-day-old plants grown under ambient temperature (AT, 24 °C/18 °C - blue background) and high-temperature (HT, 30 °C/24 °C - yellow background). Expression levels are relative to MM – AT condition. $n =$ at least three biological replicates. Each bar represents mean \pm SE. Different letters indicate statistically significant differences according to Fisher's multiple comparison test ($p < 0.05$). Gene is denoted according to the abbreviation: *GGPS1*, GERANYLGERANYL PHOSPHATE SYNTHASE 1.

285 in MM counterparts. Interestingly, an enhanced reduction was observed in the *phyAB1B2*
 286 triple mutant, which displayed similar total fruit carotenoid levels under both temperature
 287 regimes (Figure 5A). High-performance liquid chromatography (HPLC) carotenoid
 288 profiling revealed that accumulation of lycopene, alongside its precursors phytoene and
 289 phytofluene, was reduced by HT compared to AT in all genotypes aside from in the triple
 290 *phyAB1B2* mutant, which showed similar profiles of phytoene, phytofluene, and lycopene
 291 in fruits developed under both temperature regimes (Supplemental Figure S6 and Figure
 292 5B).

293 To investigate whether the temperature-mediated reduction in carotenoid content is a
 294 consequence of the transcriptional regulation of carotenoid biosynthetic genes, we further
 295 profiled *GGPS2*, *PSY1*, and *PDS* mRNA abundances in MM and the *phyAB1B2* triple
 296 mutant. In agreement with enhanced carotenoid biosynthesis during ripening, the three
 297 analyzed genes displayed a clear induction in MM under AT at the onset of ripening (from
 298 mature green to breaker stages). At the mature green stage, no significant difference in
 299 expression was observed attributable to genotype or temperature treatment. However, at

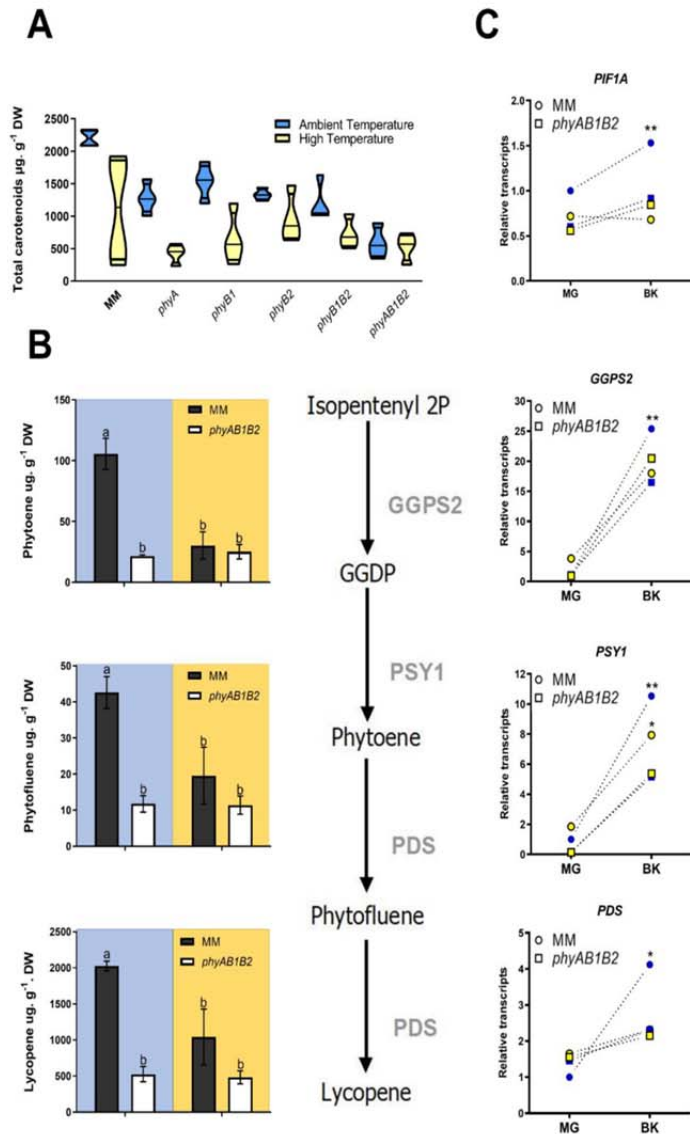


Figure 5. PHYA/B1/B2-dependent temperature perception transcriptionally regulates fruit carotenogenesis. (A) Total carotenoid (phytoene, phytofluene, lycopene, lutein and β -carotene) levels quantified from ripe fruits of Moneymaker (MM) and *phyA*, *phyB1*, *phyB2*, *phyB1B2* and *phyAB1B2* mutant plants grown under ambient (AT, blue, day/night 24 °C/18 °C) and high-temperature (HT, yellow, day/night 30 °C/24 °C). (B) Center: schematic model of lycopene biosynthetic pathway, the dotted line represents more than one enzymatic step. Left: levels of lycopene, phytoene and phytofluene in ripe fruits. AT: blue background; HT: yellow background. Each bar represents mean \pm SE. Different letters indicate statistically significant differences according to Fisher's multiple comparison test ($p < 0.05$). Right: Relative mRNA levels from carotenoids biosynthetic genes *GGPS2*, *PSY1* and *PDS* in fruits at mature green (MG) and breaker (BK) stages harvested from plants grown at AT (blue) and HT (yellow). Transcripts levels are expressed relative to MM MG – AT condition. Asterisks (* $p < 0.05$, ** $p < 0.01$) indicate differences in the analysis of variance in a multiple comparison test within the same fruit stage. Metabolites and genes are denoted according to the following abbreviations: GGDP, geranylgeranyl diphosphate; *GGPS2*, GERANYLGERANYL PHOSPHATE SYNTHASE 2; *PSY1*, PHYTOENE SYNTHASE 1; *PDS*, PHYTOENE DESATURASE. (C) Relative mRNA levels of *PIF1a* carotenogenesis regulator gene in fruits at mature green (MG) and breaker (BK) stages harvested from plants grown at AT (blue) and HT (yellow). Transcripts levels are expressed relative to MM MG – AT condition. Asterisks (** $p < 0.01$) indicate differences in the analysis of variance in a multiple comparison test within the same fruit stage.

300 breaker stage, *GGPS2*, *PSY1*, and *PDS* mRNA levels were downregulated in response to

301 both temperature and the triple *phyAB1B2* mutation (Figure 5B). The role of PIF1a in
302 tomato fruit carotenogenesis has been previously reported. Although, upon induction of
303 ripening, *PIF1a* transcript levels increased; concomitantly, Chl degradation alters the
304 quality of the light filtered through the fruit pericarp, increasing the relative red/far-red
305 ratio. As a consequence, PIF degradation increases, enhancing *PSY1* expression and
306 carotenoid accumulation (Llorente et al., 2016). Indeed, our results revealed PIF1a
307 upregulation from MG to BK stage in MM grown under AT, but its levels remained
308 invariable in both genotypes under HT (Figure 5C).

309 In summary, the temperature-insensitive phenotype observed in the *phyAB1B2* triple-
310 mutant fruits revealed that the inductive effect of PHYA/B1/B2 over the transcription of
311 carotenogenesis-associated genes is abolished by HT conditions.

312 In order to mitigate the influence of any possible pleiotropic effect of *phy* mutations at the
313 whole-plant level, we further analyzed fruit carotenoid accumulation in fruit-specific
314 *PHYA*- and *PHYB2*-silenced lines, namely *PHYA*^{RNAi} and *PHYB2*^{RNAi}. Regardless of
315 temperature, the lycopene content in *PHYA*^{RNAi} or *PHYB2*^{RNAi} fruit was reduced by half in
316 comparison to control fruits developed under AT, the latter of which were affected by HT
317 conditions (Figure 6A). It is worth noting that this effect was observed in two independent
318 transgenic lines for each genotype (Supplemental Figure S7). In agreement, *PSY1* transcript
319 accumulation accompanied the variations observed in lycopene content (Figure 6B),
320 confirming that fruit-localized PHY-mediated temperature perception controls carotenoids
321 accumulation through transcriptional regulation of the biosynthetic enzyme-encoding
322 genes.

323

324 ***PHYA*- and *PHYB2*-mediated temperature perception controls carotenoids** 325 **biosynthesis through master ripening transcription factors**

326 Besides *PIF1a* (Llorente et al., 2016), *PSY1* expression has been demonstrated to be
327 regulated by ripening-associated transcription factors in tomato (Liu et al., 2015). For this
328 reason, we profiled the mRNA levels of candidate genes encoding master ripening
329 regulators, namely *APETALA2a* (*AP2a*), *NON-RIPENING* (*NOR*), *RIPENING INHIBITOR*
330 (*RIN*), *TOMATO AGAMOUS-LIKE* (*TAGL1*), and *FRUITFULL1* and 2 (*FUL1/2*) (Klee and
331 Giovannoni, 2011), in *PHY*^{RNAi} lines subjected to both temperature regimes.

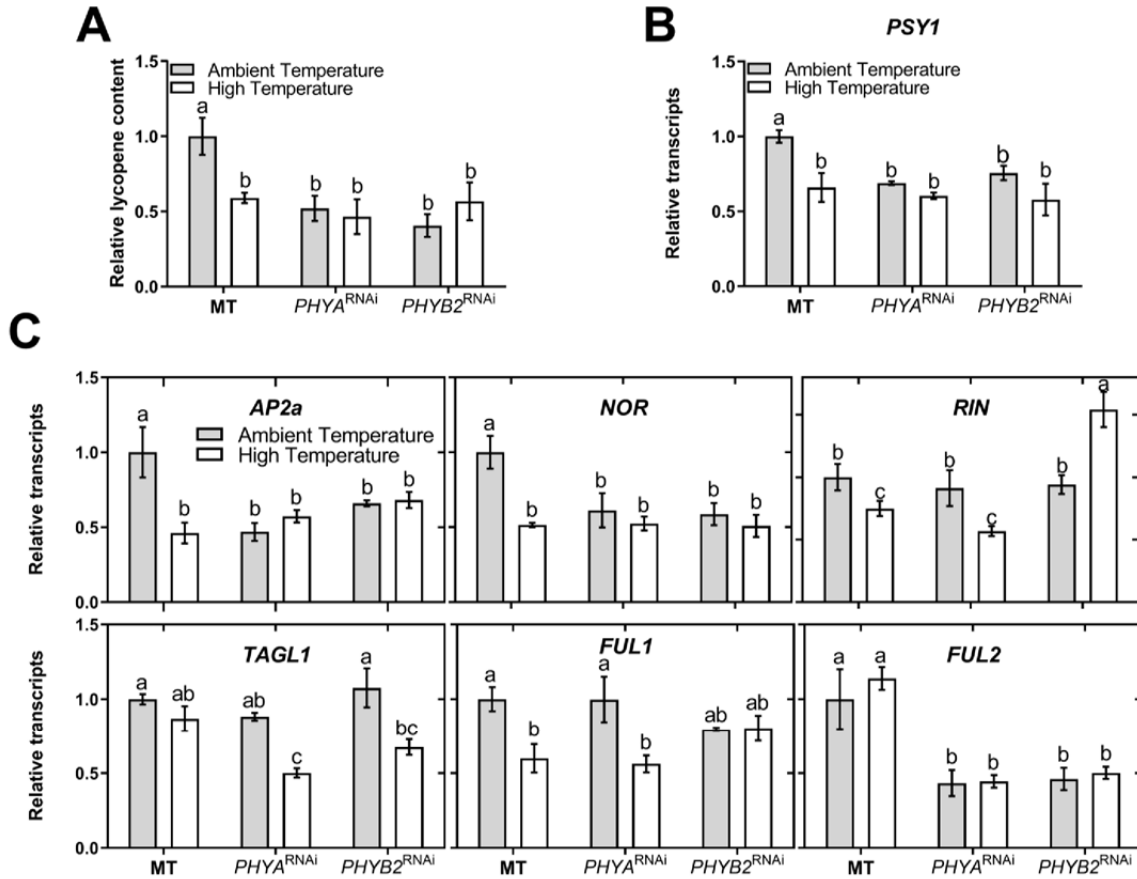


Figure 6. Fruit-localized *PHYA* and *PHYB2* are involved in temperature perception impacting lycopene synthesis and master fruit ripening regulators. (A) Lycopene levels quantified in ripe fruits from Micro-Tom (MT) control genotype and fruit-specific *PHYA*- (*PHYA*^{RNAi}) and *PHYB2*- (*PHYB2*^{RNAi}) knockdown transgenic lines grown under ambient (24 °C/18 °C) and high temperature (30 °C/24 °C). Lycopene levels were quantified and expressed relative to MT fruits at ambient temperature and values are means of at least three biological replicates from two independent lines for each genotype. Each bar represents mean ± SE. (B,C) Relative mRNA levels of (B) *PSY1* (C) and master fruit ripening regulator genes in MT, *PHYA*^{RNAi} and *PHYB2*^{RNAi} breaker fruit samples harvested under AT and HT. Expression levels are relative to MT – AT condition. n = at least three biological replicates. Each bar represents mean ± SE. Different letters indicate statistically significant differences according to Fisher’s multiple comparison test ($p < 0.05$). *RIN*; *RIPENING INHIBITOR*, *NOR*; *NON-RIPENING*, *FUL1*; *FRUITFULL1*, *FUL2*; *FRUITFULL2*, *AP2a*; *APETALA2a*, *TAGL1*; *TOMATO AGAMOUS-LIKE1*, *PSY1*; *PHYTOENE SYNTHASE 1*.

332 Three expression patterns were observed; i) *RIN*, *TAGL1*, and *FUL1* mRNA levels
 333 responded to temperature treatment and in certain cases these responses varied in the
 334 absence of *PHYA* or *PHYB2*, ii) *FUL2* was downregulated only in the lack of functional
 335 *PHYs* (*PHYA*^{RNAi} or *PHYB2*^{RNAi} lines), and iii) *AP2a* and *NOR* mRNAs displayed a clear

336 response to PHY-mediated temperature perception (Figure 6C). These results suggest that
337 fruit-localized PHY-mediated temperature perception controls carotenoid accumulation via
338 transcriptional regulation of ripening master controller genes.

339 Combined, these results decrypt the role of fruit-localized PHYA and PHYB1/B2 as
340 temperature sensors in tomato fruits, which regulate carotenoid accumulation through the
341 transcriptional control of genes involved in their biosynthesis by alternative and converging
342 molecular pathways.

343

344

345 DISCUSSION

346

347 Studies performed on plants under warm treatment or employing PHY-signalling defective
348 mutants have demonstrated the synergistic influence of light and temperature on the
349 regulation of chloroplast metabolism (Stephenson et al., 2009; Zhao et al., 2016; Spicher et
350 al., 2016; Dubreuil, et al., 2017; Spicher et al., 2017). Despite this fact, the two factors have
351 been studied independently, limiting our comprehensive understanding of light- and
352 temperature-perception mechanisms at the molecular level. Recently, the role of PHYs as
353 thermosensors by the gradual inactivation of PHYB by increasing temperature was reported
354 in *A. thaliana* (Legris et al., 2017). However, whether this mechanism operates in crop
355 species evolved in different environments, and how this PHY-dependent temperature
356 signaling cascade impacts major metabolic pathways, remains poorly understood. It is
357 worth mentioning that PHY-independent temperature responses have also been described
358 associated with other photoreceptors (Fujii et al., 2017; Ma et al., 2016) and also in
359 photoreceptor-impaired conditions (Legris et al., 2016). In accordance, we also observed
360 PHY-independent temperature responses here (Figure 2C). In the current study, we present
361 experimental evidence that central enzyme-encoding genes of Chl and carotenoid
362 metabolism are regulated at the transcriptional level by PHYB1/B2- and PHYA/B1/B2-
363 mediated temperature perception in tomato leaf chloroplasts and fruit chromoplasts,
364 respectively.

365 Constitutive HT-induced features were previously observed in the *A. thaliana phyB* loss-of-
366 function mutant (Jung et al., 2016; Huang et al., 2019). In contrast to the single-copy gene
367 *PHYB* found in *A. thaliana* (Sharrock and Quail, 1989), the tomato genome harbors two
368 *PHYB* paralogs, *PHYB1* and *PHYB2*, which originated during a genome triplication event
369 in the Solanaceae common ancestor (Tomato Genome Consortium, 2012). Indeed, results
370 from our current work indicate that loss-of-function in the double *phyB1B2* mutant, rather
371 than single *phyB1* or *phyB2* mutations, is necessary to generate a thermoinsensitive
372 phenotype in tomato leaves leading to a reduction in Chl content, indicating that PHYB1
373 and PHYB2 play additive functions as temperature sensors (Figure 1B). The *phyB1B2*
374 double mutant did not show changes in the mRNA abundances of Chl biosynthetic genes in
375 response to HT (Figure 1D). However, these genes were upregulated by HT in MM leaves,

376 which does not explain the low-Chl phenotype shown by these plants (Figure 1B) and
377 suggests a highly complex regulatory mechanism.

378 Interestingly, together with the reduction in Chl content, increased Chl fluorescence
379 parameters were registered (Figure 1C). Our results are consistent with the finding in *A.*
380 *thaliana* that faster electron transport occurred under HT conditions acting as an electron
381 sink for the increment in photorespiration (Zhang and Sharkey, 2009).

382 The observable decrease in total Chl has been associated with a decrease in the LHCII,
383 serving as a protective mechanism in plants undergoing abiotic stress (Ishida et al., 2000).

384 In agreement, we observed a reduction in chloroplast number and alterations in grana
385 stacking (Figure 2), probably mediated by higher *PIF3* mRNA level in response to

386 *PHYB1B2*-mediated temperature inactivation (Supplemental Figure S4A). In line with this,
387 *PIF3* protein accumulation led to impaired chloroplast development in *A. thaliana*

388 (Stephenson et al., 2009). Moreover, our results provide genetic evidence that HT and the
389 *phyB1B2* mutation trigger Chl catabolism via the upregulation of genes associated with Chl

390 degradation, i.e., *CLH4*, *PPH*, *SGR-like*, and *PAO* (Figure 3). It was recently demonstrated
391 that *PIF4* regulates senescence in tomato (Rosado et al., 2019). Additionally, *PHYs* trigger

392 *PIF4* degradation (Lorrain et al., 2008), avoiding its inductive role on Chl breakdown
393 (Sakuraba et al., 2014; Song et al., 2014; Zhang et al., 2015). In this sense, several

394 canonical *PIF* binding motifs, i.e., G- and PBE-box (Martínez-García et al., 2000; Zhang et
395 al., 2013), were found in the promoter of the Chl degrading-associated genes mentioned

396 above (Supplemental Figure S4B). Further reports extensively associate the inhibition of
397 *PIF4* degradation in response to HT impacting several events throughout the plant cycle

398 (Koini et al., 2009; Qiu et al., 2019; Zhou et al., 2019). Together, these data suggest that
399 inactivation of *PHYB1/B2* under HT affects Chl accumulation through altered chloroplast

400 biogenesis (Figure 2) and degradation (Figure 3), likely via *PIF1b/PIF3*- and *PIF4*-
401 dependent mechanism(s), respectively.

402 Our findings additionally indicate a down-regulation of *GGPS1* mRNA levels by
403 temperature and the *phyB1B2* mutation (Figure 4B). Since GGPS is the last shared step

404 between the Chl and carotenoid biosynthetic pathways (Cordoba et al., 2009), this result is
405 in accordance with the impairment of Chl and carotenoid synthesis in the leaves under these

406 conditions (Figure 2B,4A).

407 Besides the impact on vegetative organs, our data also indicated that HT negatively
408 influences carotenoid accumulation in tomato fruits (Figure 5A). Alterations of isoprenoid-
409 derived compounds in response to thermal stress have been increasingly demonstrated over
410 the last years (Velikova et al., 2011; Spicher et al., 2016). Exposure of single, double, and
411 triple PHY mutants as well as the MM control plants to two independent temperature
412 regimes revealed a combinatory effect of temperature and the action of PHYs on carotenoid
413 content of ripe fruits (Figure 5A). In contrast to the other genotypes analyzed, the reduced
414 levels of fruit lycopene and their precursors observed in *phyAB1B2* might be due to
415 impaired temperature perception in this genotype (Figure 5B). Consistent with this view,
416 our findings indicate that the *phyAB1B2* mutations, as well as HT conditions, downregulate
417 the expression of the major carotenoid biosynthetic genes, *e.g.*, *GGPS2*, *PSY1*, and *PDS*
418 (Figure 5B). This is in agreement with our previous report showing that these genes are
419 transcriptionally regulated by PHY-mediated light perception in tomato fruit (Bianchetti et
420 al., 2018).

421 To further examine whether the observed impact on fruit carotenoids was the effect of
422 whole-plant PHY deficiency or those localized in the fruits, we analyzed fruit-specific
423 RNAi *PHYA*- and *PHYB*-silenced lines in MT genetic background (Bianchetti et al., 2018).
424 Results showed equivalent reductions of lycopene accumulation and *PSY1* transcript levels
425 in both transgenic lines, showing temperature insensitivity (Figure 6A, 6B), demonstrating
426 that fruit-localized PHYs act as thermosensors and that this effect is genotype independent.
427 Indeed, the central role played by temperature and PHYs controlling *PSY1* expression
428 (Figure 6B) is supported by previous studies demonstrating that PIF1a downregulates
429 carotenoid biosynthesis via *PSY1* transcriptional repression in tomato fruits (Llorente et al.,
430 2016), similarly as its ortholog in *A. thaliana* in response to temperature (Toledo-Ortiz et
431 al., 2014). In addition to PIF1a, carotenoid biosynthesis in tomato fruit is markedly
432 regulated at the transcriptional level by the master ripening transcription factors RIN, NOR,
433 *FUL1*, *FUL2*, *TAGL1*, and *AP2a* (Klee and Giovanonni, 2011). Whereas a non-combined
434 effect of fruit-specific *PHY* expression and temperature on *RIN*, *TAGL1*, *FUL1*, or *FUL2*
435 transcript abundance was observed, *AP2a* and *NOR* mRNA levels responded to temperature
436 in a PHY-dependent manner (Figure 6C), thus contributing to a reduction in lycopene
437 content (Figure 6A), most likely by the transcriptional regulation of *PSY1*, as previously

438 described (Chung et al., 2010; Karlova et al., 2011; Yuan et al., 2016; Cruz et al., 2018).
439 These results exposed an interesting network that regulates ripening in response to light and
440 temperature in an independent or integrated way, warranting this key evolutionarily
441 selected process.

442 Overall, our results support a model (Figure 7) where increases in temperature induce the
443 inactivation of PHYs, probably through the conformational change from the biologically
444 active Pfr to the inactive Pr form. The thermosensing role of PHYB1/B2 impacts leaf Chl
445 and carotenoid levels through combined control of chloroplast biogenesis and the transcript
446 levels of carotenoid biosynthetic and Chl degrading enzyme genes. Moreover, our data
447 demonstrate that PHYA/PHYB1/PHYB2-mediated temperature perception modulates
448 carotenoid metabolism in fruit. The data also showed the involvement of master ripening
449 regulator genes as mediators of PHY-dependent temperature regulation of the carotenoid
450 biosynthetic pathway. In conclusion, this study demonstrates the effect of PHY-mediated
451 temperature perception on both photosynthetic and heterotrophic tomato plastid
452 metabolism. Moreover, the results presented here identify the PHYs as critical hubs that
453 can be manipulated to maintain and/or improve the nutritional quality of edible fruits in the
454 context of global increasing temperatures.

455

456

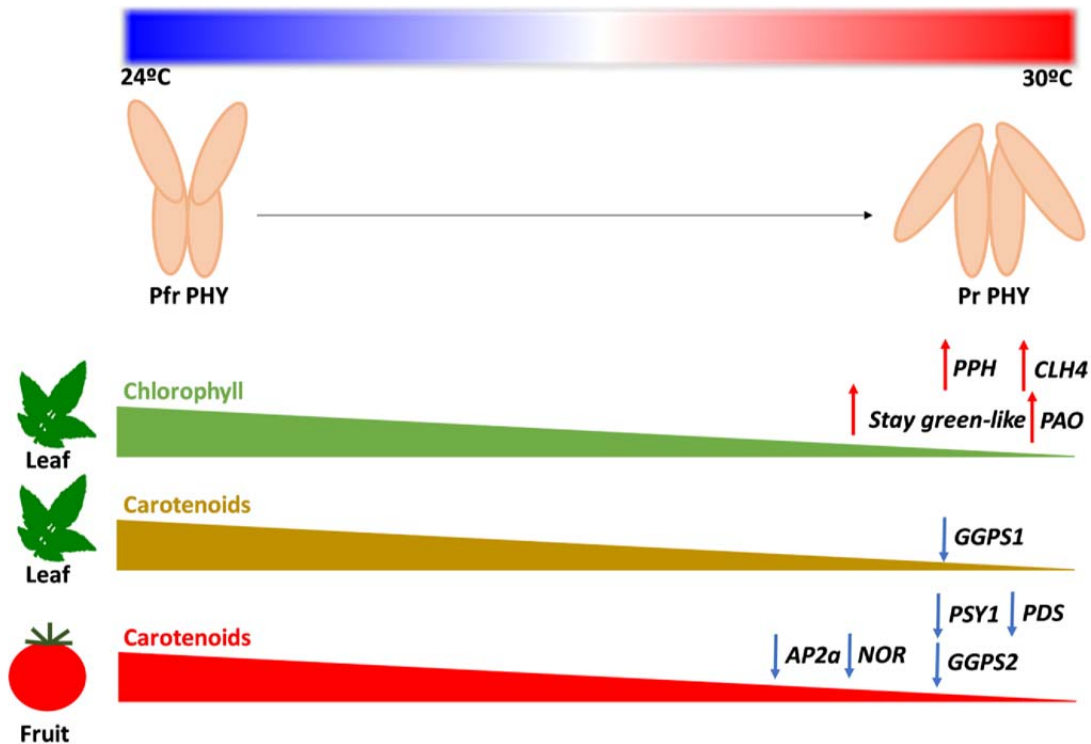


Figure 7. The effect of PHY-mediated temperature perception on tomato metabolism regulation. The rise of ambient temperature shifts balance to the inactive phytochrome (Pr) form, which promotes chlorophyll degradation pathway in source leaves through the transcriptional up-regulation of chlorophyll catabolic enzyme-associated genes. Additionally, reduced levels of Pfr impair carotenoid accumulation in both leaves and ripe fruits, through the transcriptional downregulation of carotenoid biosynthetic and master ripening regulator genes.

457 METHODS

458

459 Plant material, growth conditions, and sampling

460 *Solanum lycopersicum* plants (cv. MoneyMaker) harboring loss-of-function mutations in
 461 *phyA*, *phyB1*, *phyB2*, *phyB1B2*, and *phyAB1B2* were previously characterized (Kerckhoffs
 462 et al., 1996; Kerckhoffs et al., 1997; Lazarova et al., 1998a; Lazarova et al., 1998b;
 463 Kerckhoffs et al., 1999; Weller et al., 2000). Micro-Tom fruit-specific *PHYA*- and *PHYB2*-
 464 silenced lines (*PHYA*^{RNAi} and *PHYB2*^{RNAi}) were previously obtained and characterized by
 465 Bianchetti et al. (2018). Although the Micro-Tom cultivar is deficient in brassinosteroid
 466 biosynthesis due to the weak mutation *d*, it has been extensively demonstrated that it
 467 represents a convenient and adequate model system to study fruit biology (Campos et al.,

2010). In this work, we used Micro-Tom PHYA^{RNAi} and PHYB2^{RNAi} lines as a proof of concept that fruit-localized PHYs regulate carotenogenesis in a temperature-dependent manner in this organ and that this mechanism is genotype independent.

Tomato seeds (cv. MoneyMaker and Micro-Tom) were sown under standard greenhouse conditions (day/night 24°C/18°C, 16/8 h light/dark, and 60% air relative humidity) in Floricultura Z substrate. Twenty-day-old plants were transplanted to 9-L pots and cultivated for 120 days (16/8 h light/dark and 60% air relative humidity) in greenhouses under two distinct temperature regimens: ambient (24°C/18°C) and high (30°C/24°C) temperature with a mean daily difference of 5°C (Supplemental Figure S1A, B). These temperatures have been previously described as optimal and suboptimal high for tomato (Ayenan et al., 2019). Plants were cultivated under 250 $\mu\text{mol m}^{-2} \text{s}^{-1}$ light intensity, which is lower than the tomato saturation point (approximately 800 $\mu\text{mol m}^{-2} \text{s}^{-1}$). To avoid unwanted effects on plant water status (Fahad et al., 2017), the plants were watered twice a day and the relative ambient humidity was monitored (Supplemental Figure S1C). Leaves (seventh fully expanded leaf from bottom to top) and fruits [at mature green, breaker, and ripe (7 days after breaker) stages] from MoneyMaker background plants were harvested 65 and 80–110 days after the beginning of the temperature treatment. Fruits from Micro-Tom plants were harvested 75–90 days after the start of temperature treatment. Samples were ground in liquid N₂ and freeze-dried prior to subsequent analysis.

487

488 **Pigment quantification**

Chlorophyll (Chl) extraction was carried out from 5 mg of freeze-dried leaf tissue in 1 mL of 80:20 acetone:Tris-HCl 100 mM pH 7.5. Samples were sonicated for 5 min at 42 kHz and further centrifuged at 16000 $\times g$ for 2 min. The supernatant was collected and the procedure was repeated until the green color was totally removed from the tissue. Spectrophotometer measurements were performed at 537, 647, 663, and 750 nm. Total Chl content was estimated by the equation: 0.01373 X (A663-A750) – 0.000897 X (A537-A750) – 0.003046 X (A647-A750) (Sims and Gamon, 2003). For leaf carotenoid extraction, 5 mg of freeze-dried samples were immersed in 1 ml of *N,N*-dimethylformamide, sonicated for 5 min at 42 kHz, and centrifuged at 16000 $\times g$ for 5 min. Supernatant absorbance was recorded at 480, 647, and 664 nm, then carotenoid contents

499 were determined by the equation: $\{1000 \times A_{480} - [1.12 \times (12 \times A_{664}) - (3.11 \times A_{647})]$
500 $+ [34.07 \times (20.78 \times A_{647}) - (4.88 \times A_{664})]\} / 245$ (Wellburn, 1994). Fruit carotenoid
501 extraction was carried out from 20 mg of freeze-dried fruit tissue according to Bianchetti et
502 al., 2018. Phytoene, phytofluene, lycopene, β -carotene, and lutein were determined by
503 high-performance liquid chromatography (HPLC). Eluted compounds were detected at 450
504 nm (lycopene, β -carotene, and lutein), 286 nm (Phytoene), and 347 nm (Phytofluene) as
505 described in Fraser et al. (2000).

506

507 **Chlorophyll fluorescence measurements**

508 Chl fluorescence parameters were determined according to Lira et al. (2017) using a
509 portable open gas-exchange system (LI-6400XT system; LI-COR) equipped with an
510 integrated modulated Chl fluorometer (LI-6400-40; LI-COR). Briefly, the second leaflet of
511 the sixth fully expanded leaf from 85-day-old plants was kept under dark adaptation for 60
512 min, then weak and saturating white light pulses were applied to determine, respectively,
513 initial fluorescence and maximum fluorescence emission. Further, the same procedure was
514 applied on light-adapted leaves to determining the light-adapted initial fluorescence and
515 maximum fluorescence emission. The values were used to calculate maximum quantum
516 efficiency of PSII, PSII operating efficiency, and PSII maximum efficiency.

517

518 **Plastid abundance and ultrastructure**

519 Two-week-old MoneyMaker and *phyB1B2* plants grown under standard conditions were
520 transferred to the distinct temperature conditions described above. After one week, the
521 fourth fully expanded leaf was used for determining plastid abundance and ultrastructure
522 analysis.

523 Plastid abundance was determined in the leaf mesophyll as described in Bianchetti et al.
524 (2017). In brief, leaf samples were incubated in 3.5% glutaraldehyde for 60 min and then in
525 0.1 M Na-EDTA (pH 9.5) at 60°C for 180 min. Isolated cells were visualized through
526 optical microscopy and plastid number per cell was estimated using the ImageJ program
527 (<https://imagej.nih.gov/ij/>).

528 For ultrastructure analysis, leaf segments were fixed at 4°C in Karnovsky's solution (2.5%
529 [v/v] glutaraldehyde and 2% [v/v] paraformaldehyde in 0.1 M sodium phosphate buffer, pH

530 7.2) for 24 h. After washing in phosphate buffer, the samples were post-fixed in buffered
531 1% (w/v) osmium tetroxide, washed, dehydrated in a graded series of acetone, and
532 embedded in Spurr's resin. The resin was polymerized at 60°C. Ultrathin sections were
533 stained with saturated uranyl acetate (Watson, 1958) and lead citrate (Reynolds, 1963) and
534 observed using a JEM 1011 transmission electron microscope.

535

536 **RNA extraction and reverse transcription quantitative PCR (RT-qPCR)**

537 RNA extraction, cDNA synthesis, primer design, and qPCR assays were performed as
538 described in Quadrana et al. (2013). The primers used for RT-qPCR analyses are listed in
539 Supplementary Table S2. qPCR reactions were performed in a QStudio6 – A1769 PCR
540 Real-Time thermocycler using 2X Power SYBR Green Master Mix in a final volume of 10
541 µL. Absolute fluorescence data were analyzed using LinRegPCR software to obtain Ct and
542 primer efficiency values. Relative mRNA abundance was calculated and normalized with
543 the $\Delta\Delta C_t$ method using two reference genes (Expósito-Rodríguez et al., 2008):
544 *EXPRESSED* and *TIP4.1* for leaves and *EXPRESSED* and *CAC* for fruits (Quadrana et al.,
545 2013).

546

547 **Phylogenetic analysis**

548 Amino acid sequences of *A. thaliana* PROTOCHLOROPHYLLIDE
549 OXIDOREDUCTASES (PORA, PORB, and PORC) were BLAST against the tomato
550 genome in Sol Genomics network database (<http://solgenomics.net>). Homologous
551 sequences from *Solanum tuberosum*, *A. thaliana*, *Arapidopsis lyrata*, *Brasica oleracea*,
552 *Brasica rapa*, *Sorghum bicolor*, *Zea mays*, and *Setaria viridis* were retrieved by BLASTp
553 against Viridiplantae in Phytozome (<http://phytozome.jgi.doe.gov/pz/portal.html>).
554 MUSCLE package available in MEGA software 10.0.3 was used to perform multiple
555 sequences alignments. Phylogenetic reconstruction was performed with the maximum-
556 likelihood method with 5,000 bootstrap replications.

557

558 **Data analysis**

559 The values in the figures represent the mean of at least three biological replicates \pm
560 standard error. Statistical differences in parameters were analyzed with InfoStat/F software

561 (<http://www.infostat.com.ar>). Two-way analysis of variance (ANOVA) was performed to
562 determine genotype (G), environmental (E) or GxE interaction. A Fisher test ($p < 0.05$) was
563 performed to compare GxE interaction and a t -test ($p < 0.05$) was applied to discriminate
564 means of the sample within genotypes.

565

566 **Accession numbers**

567 Sequence data from this article can be found in the GenBank/EMBL data libraries under
568 accession numbers: AJ001913 (*phyA*); AJ002281 (*phyB1*) and AF122901 (*phyB2*).

569

570 **Supplemental Data**

571

572 **Supplemental Figure S1.** Time course of temperature and relative humidity measurements
573 registered along the plant growth cycle.

574 **Supplemental Figure S2.** Hydric status of Moneymaker and knockout-phytochrome
575 mutant plants at two temperatures regimes.

576 **Supplemental Figure S3.** Phylogenetic construction of the PROTOCHLOROPHYLLIDE
577 OXIDOREDUCTASE protein family.

578 **Supplemental Figure S4.** PHYTOCHROME INTERACTION FACTORS involvement in
579 the regulation of temperature-induced chlorophyll reduction.

580 **Supplemental Figure S5.** Expression profile of carotenoid biosynthetic genes in leaves.

581 **Supplemental Figure S6.** Carotenoid profile in ripe fruits from Moneymaker and
582 knockout- phytochrome mutants.

583 **Supplemental Figure S7.** Lycopene content in ripe fruits from fruit-specific PHYA- and
584 PHYB2-knockdown transgenic lines.

585 **Supplemental Table S1.** Relative expression of chlorophyll biosynthetic genes.

586 **Supplemental Table S2.** Primer sequences used in this study.

587

588 **Figure Legends**

589 **Figure 1. PHYB1/B2 are involved in temperature perception impacting leaf**
590 **chlorophyll metabolism and fluorescence parameters in tomato.** (A) Side view of 50-
591 day-old *S. lycopersicum* cv. Moneymaker (MM) plants and *phyB1*-, *phyB2*-, and *phyB1B2*-

592 knockout mutants grown under ambient- (AT, day/night 24°C/18°C) and high-temperature
593 (HT, day/night 30°C/24°C) conditions. (B) Quantification of total chlorophyll (Chl) in the
594 seventh fully expanded leaf from 85-day-old plants. Each bar represents mean \pm SE. (C)
595 PSII maximum efficiency (F_v'/F_m'), PSII operating efficiency (F_q'/F_m'), and maximum
596 quantum efficiency of PSII (F_v/F_m) measured in the sixth fully expanded leaf from 85-day-
597 old plants. n = at least five biological replicates. Each bar represents mean \pm SE. Different
598 letters indicate statistically significant differences according to Fisher's multiple
599 comparison test ($p < 0.05$). Asterisks (* $p < 0.05$, ** $p < 0.01$) indicate statistically significant
600 differences by two-tailed Student's t -test between MM and *phyB1B2* under the same
601 environmental conditions. (D) HT/AT relative expression ratio of *GLK1*, *GGDR*, *CHLG*,
602 *POR1*, *POR2*, and *POR3* mRNA abundance in MM and *phyB1B2*-mutant leaf samples
603 from 85-day-old plants. n = at least three biological replicates. Each bar represents mean \pm
604 SE. Asterisks (* $p < 0.05$, ** $p < 0.01$) indicate statistically significant differences by two-
605 tailed Student's t -test between AT and HT within the same genotype. Genes are denoted
606 according to the abbreviations: *GLK1*, *GOLDEN2-LIKE1*; *GGDR*, *GERANYLGERANYL*
607 *DIPHOSPHATE REDUCTASE*; *CHLG*, *CHLOROPHYLL SYNTHASE*; *POR*,
608 *PROTOCHLOROPHYLLIDE OXIDOREDUCTASE*.

609

610 **Figure 2. High temperature affects plastid biogenesis and development in leaves in a**
611 **PHYB1/B2-dependent manner.** (A) Visualization of a representative leaf from 21-day-old
612 *S. lycopersicum* cv. Moneymaker (MM) and *phyB1B2*-knockout mutants after two weeks
613 under ambient- (AT, day/night 24°C/18°C) and high-temperature (HT, 30°C/24°C)
614 conditions. Red arrows indicate chlorotic leaves (MM at HT, *phyB1B2* at AT, and *phyB1B2*
615 at HT). (B) Quantification of total Chl in leaves cultivated under AT (blue background) and
616 HT (yellow background) conditions. n = at least three biological replicates. Each bar
617 represents mean \pm SE. (C) Plastid density per mesophyll cell. Values represent chloroplast
618 quantification of ± 70 cells. Different letters indicate statistically significant differences
619 according to Fisher's multiple comparison test ($p < 0.05$). Each bar represents mean \pm SE.
620 (D) Representative TEM images of chloroplasts from MM and *phyB1B2* leaves grown
621 under AT and HT conditions. G indicates grana and DT indicates dilated thylakoids.

622

623 **Figure 3. High temperature enhances chlorophyll degradation in leaves in a**
624 **PHYB1/B2-dependent manner.** (A) Schematic model of chlorophyll (Chl) degradation
625 pathway. Enzymes and metabolites are denoted according to the following abbreviations:
626 Pheo *a*, pheophytin *a*; Chlide *a*, chlorophyllide *a*; Pheide *a*, pheophorbide *a*; RCC, red
627 chlorophyll catabolite; CLH, CHLOROPHYLLASE; SGR, STAY GREEN; SGR-like,
628 PPH, PHEOPHYTINASE; STAY GREEN-LIKE; PAO, PHEOPHORBIDE *a*
629 OXYGENASE. The enzymes highlighted in red are those that showed to be regulated by
630 temperature in a PHYB1/B2-dependent manner according to Figure 3B. (B) Relative
631 mRNA levels of Chl degrading enzyme-encoding genes in Moneymaker (MM) and
632 *phyB1B2* mutant leaf samples from 85-day-old plants grown under ambient- (AT,
633 24°C/18°C; blue background) and high-temperature (HT, 30°C/24°C; yellow background)
634 conditions. Expression levels are relative to MM – AT conditions. n = at least three
635 biological replicates. Each bar represents mean ± SE. Different letters indicate statistically
636 significant differences according to Fisher's multiple comparison test ($p < 0.05$).

637

638 **Figure 4. PHYB1/B2-dependent temperature perception transcriptionally regulates**
639 **leaf carotenogenesis.** (A) Total carotenoid levels expressed in µg per g of dry weight. n =
640 at least five biological replicates. (B) Relative mRNA levels of *GGPS1* gene in
641 Moneymaker (MM) and *phyB1B2*-mutant leaf samples from 85-day-old plants grown under
642 ambient- (AT, 24°C/18°C; blue background) and high-temperature (HT, 30°C/24°C;
643 yellow background) conditions. Expression levels are relative to MM – AT conditions. n =
644 at least three biological replicates. Each bar represents mean ± SE. Different letters indicate
645 statistically significant differences according to Fisher's multiple comparison test ($p <$
646 0.05). Gene is denoted according to the abbreviation: *GGPS1*, *GERANYLGERANYL*
647 *PHOSPHATE SYNTHASE 1*.

648

649 **Figure 5. PHYA/B1/B2-dependent temperature perception transcriptionally regulates**
650 **fruit carotenogenesis.** (A) Total carotenoid (phytoene, phytofluene, lycopene, lutein, and
651 β-carotene) levels quantified from ripe fruits of Moneymaker (MM) and *phyA*-, *phyB1*-,
652 *phyB2*-, *phyB1B2*-, and *phyAB1B2*-mutant plants grown under ambient- (AT, day/night

653 24°C/18°C; blue fill) and high-temperature (HT, day/night 30°C/24°C; yellow fill)
654 conditions. (B) Center: schematic model of the lycopene biosynthetic pathway, the dotted
655 line represents more than one enzymatic step. Left: levels of lycopene, phytoene, and
656 phytofluene in ripe fruits. AT: blue background; HT: yellow background. Each bar
657 represents mean \pm SE. Different letters indicate statistically significant differences
658 according to Fisher's multiple comparison test ($p < 0.05$). Right: Relative mRNA levels of
659 carotenoid biosynthetic genes *GGPS2*, *PSY1*, and *PDS* in fruits at mature green (MG) and
660 breaker (BK) stages harvested from plants grown under AT (blue) and HT (yellow)
661 conditions. Transcripts levels are expressed relative to MM MG – AT condition. Asterisks
662 (* $p < 0.05$, ** $p < 0.01$) indicate differences in the analysis of variance in a multiple
663 comparison test within the same fruit stage. Metabolites and genes are denoted according to
664 the following abbreviations: GGDP, geranylgeranyl diphosphate; *GGPS2*,
665 *GERANYLGERANYL PHOSPHATE SYNTHASE 2*; *PSY1*, *PHYTOENE SYNTHASE 1*;
666 *PDS*, *PHYTOENE DESATURASE*. (C) Relative mRNA levels of *PIF1a* carotenogenesis
667 regulator gene in fruits at mature green (MG) and breaker (BK) stages harvested from
668 plants grown under AT (blue) and HT (yellow) conditions. Transcripts levels are expressed
669 relative to MM MG – AT conditions. Asterisks (** $p < 0.01$) indicate differences in the
670 analysis of variance in a multiple comparison test within the same fruit stage.

671

672 **Figure 6. Fruit-localized PHYA and PHYB2 are involved in temperature perception**
673 **impacting lycopene synthesis and master fruit ripening regulators.** (A) Lycopene levels
674 quantified in ripe fruits from Micro-Tom (MT) control genotype and fruit-specific *PHYA*-
675 (*PHYA*^{RNAi}) and *PHYB2*- (*PHYB2*^{RNAi}) knockdown transgenic lines grown under ambient-
676 (24°C/18°C) and high-temperature (30°C/24°C) conditions. Lycopene levels were
677 quantified and expressed relative to MT fruits under AT conditions and values are means of
678 at least three biological replicates from two independent lines for each genotype. Each bar
679 represents mean \pm SE. (B,C) Relative mRNA levels of (B) *PSY1* (C) and master fruit
680 ripening regulator genes in MT, *PHYA*^{RNAi}, and *PHYB2*^{RNAi} breaker fruit samples harvested
681 under AT and HT conditions. Expression levels are relative to MT – AT conditions. n = at
682 least three biological replicates. Each bar represents mean \pm SE. Different letters indicate
683 statistically significant differences according to Fisher's multiple comparison test ($p <$

684 0.05). *RIN*; *RIPENING INHIBITOR*, *NOR*; *NON-RIPENING*, *FUL1*; *FRUITFULL1*, *FUL2*;
685 *FRUITFULL2*, *AP2a*; *APETALA2a*, *TAGL1*; *TOMATO AGAMOUS-LIKE1*, *PSY1*;
686 *PHYTOENE SYNTHASE 1*.

687

688 **Figure 7. The effect of PHY-mediated temperature perception on tomato metabolism**

689 **regulation.** The rise of ambient temperature shifts balance to the inactive phytochrome (Pr)
690 form, which promotes the Chl degradation pathway in source leaves through the
691 transcriptional up-regulation of Chl catabolic enzyme-associated genes. Additionally,
692 reduced levels of Pfr impair carotenoid accumulation in both leaves and ripe fruits, through
693 the transcriptional downregulation of carotenoid biosynthetic and master ripening regulator
694 genes.

695

696

Parsed Citations

- Alba R, Cordonnier-Pratt MM, Pratt LH. (2000a).** Fruit-localized phytochromes regulate lycopene accumulation independently of ethylene production in tomato. *Plant Physiology* 123: 363–370.
Pubmed: [Author and Title](#)
Google Scholar: [Author Only Title Only Author and Title](#)
- Alba R, Kelmenson PM, Cordonnier-Pratt MM, Pratt LH. (2000b).** The phytochrome gene family in tomato and the rapid differential evolution of this family in angiosperms. *Molecular Biology and Evolution* 17: 362–373.
Pubmed: [Author and Title](#)
Google Scholar: [Author Only Title Only Author and Title](#)
- Almeida J, Asis R, Molineri VN, Sestari I, Lira BS, Carrari F, Peres LEP, Rossi M. (2015).** Fruits from ripening impaired, chlorophyll degraded and jasmonate insensitive tomato mutants have altered tocopherol content and composition. *Phytochemistry* 111: 72–83.
Pubmed: [Author and Title](#)
Google Scholar: [Author Only Title Only Author and Title](#)
- Alves FRR, Lira BS, Pikart FC, Monteiro SS, Furlan CM, Purgatto E, Pascoal GB, Andrade SCS, Demarco D, Rossi M, Freschi L. (2020).** Beyond the limits of photoperception: constitutively active PHYTOCHROME B2 overexpression as a means of improving fruit nutritional quality in tomato. *Plant Biotechnology Journal* <https://doi.org/10.1111/pbi.13362>.
Pubmed: [Author and Title](#)
Google Scholar: [Author Only Title Only Author and Title](#)
- Ayenan MAT, Danquah A, Hanson P, Ampomah-Dwamena C, Sodedji FAK, Asante IK, Danquah EY. (2019)** Accelerating Breeding for Heat Tolerance in Tomato (*Solanum lycopersicum* L.: An Integrated Approach. *Agronomy* 9: 720.
Pubmed: [Author and Title](#)
Google Scholar: [Author Only Title Only Author and Title](#)
- Bianchetti RE, Cruz AB, Oliveira BS, Demarco D, Purgatto E, Peres LEP, Rossi M, Freschi L. (2017).** Phytochromobilin deficiency impairs sugar metabolism through the regulation of cytokinin and auxin signaling in tomato fruits. *Scientific Reports* 7: 7822.
Pubmed: [Author and Title](#)
Google Scholar: [Author Only Title Only Author and Title](#)
- Bianchetti RE, Lira BS, Monteiro SS, Demarco D, Purgatto E, Rothan C, Rossi M, Freschi L. (2018).** Fruit-localized phytochromes regulate plastid biogenesis, starch synthesis, and carotenoid metabolism in tomato. *Journal of Experimental Botany* 69: 3573–3586.
Pubmed: [Author and Title](#)
Google Scholar: [Author Only Title Only Author and Title](#)
- Bitá CE, Gerats T. (2013).** Plant tolerance to high temperature in a changing environment: scientific fundamentals and production of heat stress-tolerant crops. *Frontiers in Plant Science* 4: 273.
Pubmed: [Author and Title](#)
Google Scholar: [Author Only Title Only Author and Title](#)
- Box MS, Huang BE, Domijan M, Jaeger KE, Khattak AK, Yoo SJ, Sedivey EL, Jones DM, Hearn TJ, Webb ARR, Grant A, Locke JCW, Wigge PA. (2015).** ELF3 controls thermoresponsive growth in *Arabidopsis*. *Current Biology* 25: 194–199.
Pubmed: [Author and Title](#)
Google Scholar: [Author Only Title Only Author and Title](#)
- Burgie ES, Vierstra RD. (2014).** Phytochromes: An Atomic Perspective on Photoactivation and Signaling. 26: 4568–4583.
Pubmed: [Author and Title](#)
Google Scholar: [Author Only Title Only Author and Title](#)
- Campos ML, Carvalho RF, Benedito VA, Peres LEP. (2010).** The Micro-Tom model system as a tool to discover novel hormonal functions and interactions. *Plant Signaling & Behavior* 5: 267-270.
Pubmed: [Author and Title](#)
Google Scholar: [Author Only Title Only Author and Title](#)
- Chung MY, Vrebalov J, Alba R, Lee J, McQuinn R, Chung JD, Klein P, Giovannoni J. (2010).** A tomato (*Solanum lycopersicum*) *APETALA2/ERF* gene, *SIAP2a*, is a negative regulator of fruit ripening. *Plant Journal* 64: 936–947.
Pubmed: [Author and Title](#)
Google Scholar: [Author Only Title Only Author and Title](#)
- Cordoba E, Salmi M, León P. (2009).** Unravelling the regulatory mechanisms that modulate the MEP pathway in higher plants. *Journal of Experimental Botany* 60: 2933–2943.
Pubmed: [Author and Title](#)
Google Scholar: [Author Only Title Only Author and Title](#)
- Cruz AB, Bianchetti RE, Alves FRR, Purgatto E, Peres LEP, Rossi M, Freschi L. 2018.** Light, Ethylene and Auxin Signaling Interaction Regulates Carotenoid Biosynthesis During Tomato Fruit Ripening. *Frontiers in Plant Science* 9: 1370.
Pubmed: [Author and Title](#)
Google Scholar: [Author Only Title Only Author and Title](#)
- Dubreuil C, Ji Y, Strand Å, Grönlund A. (2017).** A quantitative model of the phytochrome-PIF light signalling initiating chloroplast development. *Scientific Reports* 7: 13884.
Pubmed: [Author and Title](#)
Google Scholar: [Author Only Title Only Author and Title](#)

Pubmed: [Author and Title](#)

Google Scholar: [Author Only Title Only Author and Title](#)

Expósito-Rodríguez M, Borges AA, Borges-Pérez A, Pérez JA (2008). Selection of internal control genes for quantitative real-time RT-PCR studies during tomato development process. *BMC Plant Biology* 8: 131.

Pubmed: [Author and Title](#)

Google Scholar: [Author Only Title Only Author and Title](#)

Fahad S, Bajwa AA, Nazir U, Anjum SA, Farooq A, Zohaib A, Sadia S, Nasim W, Adkins S, Saud S, Ihsan MZ, Alharby H, Wu C, Wang D, Huang J. (2017). Crop Production under Drought and Heat Stress: Plant Responses and Management Options. *Frontiers in Plant Science*. 8: 1147.

Pubmed: [Author and Title](#)

Google Scholar: [Author Only Title Only Author and Title](#)

Fraser PD, Pinto M, Holloway DE, Bramley P. (2000). Application of high-performance liquid chromatography with photodiode array detection to the metabolic profiling of plant isoprenoids. *The Plant Journal* 24: 551-558.

Pubmed: [Author and Title](#)

Google Scholar: [Author Only Title Only Author and Title](#)

Fujii Y, Tanaka H, Konno N, Ogasawara Y, Hamashima N, Tamura S, Hasegawa S, Hayasaki Y, Okajima K, Kodama T. (2017). Phototropin perceives temperature based on the lifetime of its photoactivated state. *Proceedings of the National Academy of Sciences* 114: 9206–9211.

Pubmed: [Author and Title](#)

Google Scholar: [Author Only Title Only Author and Title](#)

Gramegna G, Rosado D, Carranza APS, Cruz AB, Simon-Moya M, Llorente B, Rodríguez-Concepción, M, Freschi L, Rossi M. (2018). PHYTOCHROME - INTERACTING FACTOR 3 mediates light - dependent induction of tocopherol biosynthesis during tomato fruit ripening. *Plant Cell & Environment* 42: 1328–1399.

Pubmed: [Author and Title](#)

Google Scholar: [Author Only Title Only Author and Title](#)

Gupta SK, Sharma S, Santisree P, Kilambi HV, Appenroth K, Sreelakshmi Y, Sharma R. (2014). Complex and shifting interactions of phytochromes regulate fruit development in tomato. *Plant, Cell and Environment* 37: 1688–1702.

Pubmed: [Author and Title](#)

Google Scholar: [Author Only Title Only Author and Title](#)

Guyer L, Hofstetter SS, Christ B, Lira BS, Rossi M, Hörtensteiner S. (2014). Different Mechanisms Are Responsible for Chlorophyll Dephytylation during Fruit Ripening and Leaf Senescence in Tomato. *Plant Physiology* 166: 44–56.

Pubmed: [Author and Title](#)

Google Scholar: [Author Only Title Only Author and Title](#)

Hörtensteiner S. (2013). Update on the biochemistry of chlorophyll breakdown. *Plant Molecular Biology* 82: 505–517.

Pubmed: [Author and Title](#)

Google Scholar: [Author Only Title Only Author and Title](#)

Huang H, McLoughlin KE, Sorkin ML, Burgie ES, Bindbeutel RK, Vierstra RD, Nusinow DA (2019). PCH1 regulates light, temperature, and circadian signaling as a structural component of phytochrome B-photobodies in *Arabidopsis*. *Proceedings of the National Academy of Sciences* 116: 8603–8608.

Pubmed: [Author and Title](#)

Google Scholar: [Author Only Title Only Author and Title](#)

Inagaki N, Kinoshita K, Kagawa T, Tanaka A, Ueno O, Shimada H, Takano M. (2015). Phytochrome B Mediates the Regulation of Chlorophyll Biosynthesis through Transcriptional Regulation of CHH and GUN4 in Rice Seedlings. *PLoS ONE* 10: 10.1371/journal.pone.0135408.

Pubmed: [Author and Title](#)

Google Scholar: [Author Only Title Only Author and Title](#)

Ishida A, Toma T, Marjenah M. (2000) Leaf gas exchange and canopy structure under wet and drought years in *Macaranga conifera*, a tropical pioneer tree. *Rainforest Ecosystems of East Kalimantan* 140:129-42.

Pubmed: [Author and Title](#)

Google Scholar: [Author Only Title Only Author and Title](#)

Jung JH, Domijan M, Klose C, Biswas S, Ezer D, Gao M, Khattak AK, Box MS, Charoensawan V, Cortijo S, Kumar M, Grant A, Locke JC, Schäfer E, Jaeger KE, Wigge PA (2016). Phytochromes function as thermosensors in *Arabidopsis*. *Science* 354: 886–889.

Pubmed: [Author and Title](#)

Google Scholar: [Author Only Title Only Author and Title](#)

Karlova R, Rosin FM, Busscher-Lange J, Parapunova V, Do PT, Fernie AR, Fraser PD, Baxter C, Angenent GC, de Maagd RA (2011). Transcriptome and Metabolite Profiling Show That APETALA2a Is a Major Regulator of Tomato Fruit Ripening. *The Plant Cell* 23: 923–941.

Pubmed: [Author and Title](#)

Google Scholar: [Author Only Title Only Author and Title](#)

Kerckhoffs LHJ, Kelmenson PM, Schreuder MEL, Kendrick CI, Kendrick RE, Hanhart CJ, Koornneef M, Pratt LH, Cordonnier-Pratt MM.

(1999). Characterization of the gene encoding the apoprotein of phytochrome B2 in tomato, and identification of molecular lesions in two mutant alleles. *Molecular and General Genetics* 261: 901–907.

Pubmed: [Author and Title](#)

Google Scholar: [Author Only](#) [Title Only](#) [Author and Title](#)

Kerckhoffs LHJ, Schreuder MEL, VanTuinen A, Koornneef M, Kendrick RE. (1997). Phytochrome control of anthocyanin biosynthesis in tomato seedlings: Analysis using photomorphogenic mutants. *Photochemistry and Photobiology* 65: 374–381.

Pubmed: [Author and Title](#)

Google Scholar: [Author Only](#) [Title Only](#) [Author and Title](#)

Kerckhoffs LHJ, Van Tuinen A, Hauser BA, Cordonnier Pratt MM, Nagatani A, Koornneef M, Pratt LH, Kendrick RE. (1996). Molecular analysis of tri-mutant alleles in tomato indicates the Tri locus is the gene encoding the apoprotein of phytochrome B1. *Planta* 199: 152–157.

Pubmed: [Author and Title](#)

Google Scholar: [Author Only](#) [Title Only](#) [Author and Title](#)

Kim K, Jeong J, Kim J, Lee N, Kim ME, Lee S, Kim SC, Choi G. (2016). PIF1 regulates plastid development by repressing photosynthetic genes in the endodermis. *Mol. Plant* 9: 1415–1427

Pubmed: [Author and Title](#)

Google Scholar: [Author Only](#) [Title Only](#) [Author and Title](#)

Klee HJ, Giovannoni JJ. (2011). Genetics and Control of Tomato Fruit Ripening and Quality Attributes. *Annual Review of Genetics* 45: 41–59.

Pubmed: [Author and Title](#)

Google Scholar: [Author Only](#) [Title Only](#) [Author and Title](#)

Koini MA, Avey L, Allen T, Tilley CA, Harberd NP, Whitelam GC, Franklin KA (2009). Report High Temperature-Mediated Adaptations in Plant Architecture Require the bHLH Transcription Factor PIF4. *Current Biology* 19: 408–413.

Pubmed: [Author and Title](#)

Google Scholar: [Author Only](#) [Title Only](#) [Author and Title](#)

Lazarova GI, Kerckhoffs LHJ, Brandstädter J, Matsui M, Kendrick RE, Cordonnier-Pratt MM, Pratt LH. (1998a). Molecular analysis of PHYA in wild-type and phytochrome A-deficient mutants of tomato. *Plant Journal* 14: 653–662.

Pubmed: [Author and Title](#)

Google Scholar: [Author Only](#) [Title Only](#) [Author and Title](#)

Lazarova GI, Kubota T, Frances S, Peters JL, Hughes MJ, Brandstadter J, Széll M, Matsui M, Kendrick RE, Cordonnier-Pratt MM, Pratt LH. (1998b). Characterization of tomato PHYB1 and identification of molecular defects in four mutant alleles. *Plant Molecular Biology* 38: 1137–1146.

Pubmed: [Author and Title](#)

Google Scholar: [Author Only](#) [Title Only](#) [Author and Title](#)

Legris M, Klose C, Burgie ES, Rojas CCR, Neme M, Hiltbrunner A, Wigge PA, Schäfer E, Vierstra RD, Casal JJ. (2016). Phytochrome B integrates light and temperature signals in Arabidopsis. *Science* 354: 897–900.

Pubmed: [Author and Title](#)

Google Scholar: [Author Only](#) [Title Only](#) [Author and Title](#)

Legris M, Nieto C, Sellaro R, Prat S, Casal JJ. (2017). Perception and signalling of light and temperature cues in plants. *Plant Journal* 90: 683–697.

Pubmed: [Author and Title](#)

Google Scholar: [Author Only](#) [Title Only](#) [Author and Title](#)

Lira BS, Gramegna G, Trench B, Alves FRR, Silva EM, Silva GFF, Thirulmalaikumar VP, Lupi ACD, Demarco D, Purgatto E, Nogueira FTS, Balazadeh S, Freschi L, Rossi M. (2017). Manipulation of a senescence-associated gene improves fleshy fruit yield. *Plant Physiology* 175: 77–91.

Pubmed: [Author and Title](#)

Google Scholar: [Author Only](#) [Title Only](#) [Author and Title](#)

Lira BS, de Setta N, Rosado D, Almeida J, Freschi L, Rossi M. (2014). Plant degreening: Evolution and expression of tomato (*Solanum lycopersicum*) dephytylation enzymes. *Gene* 546: 359–366.

Pubmed: [Author and Title](#)

Google Scholar: [Author Only](#) [Title Only](#) [Author and Title](#)

Liu L, Shao Z, Zhang M, Wang Q. (2015). Regulation of carotenoid metabolism in tomato. *Molecular Plant* 8: 28–39.

Pubmed: [Author and Title](#)

Google Scholar: [Author Only](#) [Title Only](#) [Author and Title](#)

Llorente B, D'Andrea L, Ruiz-Sola MA, Botterweg E, Pulido P, Andilla J, Loza-Alvarez P, Rodriguez-Concepcion M. (2016). Tomato fruit carotenoid biosynthesis is adjusted to actual ripening progression by a light-dependent mechanism. *Plant Journal* 85: 107–119.

Pubmed: [Author and Title](#)

Google Scholar: [Author Only](#) [Title Only](#) [Author and Title](#)

Lorrain S, Allen T, Duek PD, Whitelam GC, Fankhauser C. (2008). Phytochrome-mediated inhibition of shade avoidance involves degradation of growth-promoting bHLH transcription factors. *Plant Journal* 53: 312–323.

- Pubmed: [Author and Title](#)
Google Scholar: [Author Only Title Only Author and Title](#)
- Ma D, Li X, Guo Y, Chu J, Fang S, Yan C, Noel JP, Liu H. (2016). Cryptochrome 1 interacts with PIF4 to regulate high temperature-mediated hypocotyl elongation in response to blue light. *Proceedings of the National Academy of Sciences* 113: 224–229.**
Pubmed: [Author and Title](#)
Google Scholar: [Author Only Title Only Author and Title](#)
- Martin G, Leivar P, Ludevid D, Tepperman JM, Quail PH, Monte E. (2016). Phytochrome and retrograde signalling pathways converge to antagonistically regulate a light-induced transcriptional network. *Nature Communications* 7: 11431.**
Pubmed: [Author and Title](#)
Google Scholar: [Author Only Title Only Author and Title](#)
- Martínez-García JF, Huq E, Quail PH. (2000). Direct Targeting of Light Signals to a Promoter. *Science* 288: 859–859.**
Pubmed: [Author and Title](#)
Google Scholar: [Author Only Title Only Author and Title](#)
- Nakamura H, Muramatsu M, Hakata M, Ueno O, Nagamura Y, Hirochika H, Takano M, Ichikawa H, (2009). Ectopic overexpression of the transcription factor OsGLK1 induces chloroplast development in non-green rice cells. *Plant Cell Physiology* 50: 1933–1949.**
Pubmed: [Author and Title](#)
Google Scholar: [Author Only Title Only Author and Title](#)
- Nguyen C V, Vrebalov JT, Gapper NE, Zheng Y, Zhong S, Fei Z, Giovannoni JJ. (2014). Tomato GOLDEN2-LIKE Transcription Factors Reveal Molecular Gradients That Function during Fruit Development and Ripening. *Plant Cell* 26: 585–601.**
Pubmed: [Author and Title](#)
Google Scholar: [Author Only Title Only Author and Title](#)
- Oh S, Montgomery BL. (2014). Phytochrome-dependent coordinate control of distinct aspects of nuclear and plastid gene expression during anterograde signaling and photomorphogenesis. *Frontiers in Plant Science* 5: 171.**
Pubmed: [Author and Title](#)
Google Scholar: [Author Only Title Only Author and Title](#)
- Park E, Kim Y, Choi G. (2018). Phytochrome B Requires PIF Degradation and Sequestration to Induce Light Responses across a Wide Range of Light Conditions. *Plant Cell* 30: 1277–1292.**
Pubmed: [Author and Title](#)
Google Scholar: [Author Only Title Only Author and Title](#)
- Qiu Y, Li M, Kim RJ, Moore CM, Chen M. (2019). Daytime temperature is sensed by phytochrome. *Nature Communications* 10: 140.**
Pubmed: [Author and Title](#)
Google Scholar: [Author Only Title Only Author and Title](#)
- Quadrana L, Almeida J, Otaiza SN, Duffy T, Corrêa da Silva JV, de Godoy F, Asís R, Bermúdez L, Fernie AR, Carrari F, Rossi M. (2013). Transcriptional regulation of tocopherol biosynthesis in tomato. *Plant Molecular Biology* 81: 309–325.**
Pubmed: [Author and Title](#)
Google Scholar: [Author Only Title Only Author and Title](#)
- Reynolds ES. (1963). The use of lead citrate at high pH as an electron-opaque stain in electron microscopy. *The Journal of Cell Biology* 17: 208–212.**
Pubmed: [Author and Title](#)
Google Scholar: [Author Only Title Only Author and Title](#)
- Rockwell NC, Su Y-S, Lagarias JC. (2006). Phytochrome Structure and Signaling Mechanisms. *Annual Review of Plant Biology* 57: 837–858.**
Pubmed: [Author and Title](#)
Google Scholar: [Author Only Title Only Author and Title](#)
- Rosado D, Gramegna G, Cruz A, Lira BS, Freschi L, De Setta N, Rossi M. (2016). Phytochrome Interacting Factors (PIFs) in *Solanum lycopersicum*: Diversity, evolutionary history and expression profiling during different developmental processes. *PLoS ONE* 11: 10.1371/journal.pone.0165929.**
Pubmed: [Author and Title](#)
Google Scholar: [Author Only Title Only Author and Title](#)
- Rosado D, Trench B, Bianchetti R, Zuccarelli R, Alves FRR, Purgatto E, Floh EIS, Nogueira FTS, Freschi L, Rossi M. (2019). Downregulation of PHYTOCHROME-INTERACTING FACTOR 4 influences plant development and fruit production. *Plant Physiology* 181: 1360–1370.**
Pubmed: [Author and Title](#)
Google Scholar: [Author Only Title Only Author and Title](#)
- Saidi Y, Finka A, Goloubinoff, P. (2017). Heat perception and signalling in plants: a tortuous path to thermotolerance. *New Phytologist* 190: 556–565.**
Pubmed: [Author and Title](#)
Google Scholar: [Author Only Title Only Author and Title](#)
- Sakuraba Y, Jeong J, Kang MY, Kim J, Paek NC, Choi G. (2014). Phytochrome-interacting transcription factors PIF4 and PIF5 induce leaf senescence in *Arabidopsis*. *Nature Communications* 5: 4636.**

Pubmed: [Author and Title](#)
Google Scholar: [Author Only Title Only Author and Title](#)

Sharrock RA, Quail PH. (1989). Novel phytochrome sequences in Arabidopsis thaliana: structure, evolution, and differential expression of a plant regulatory photoreceptor family. Genes & Development 3: 1745–1757.

Pubmed: [Author and Title](#)
Google Scholar: [Author Only Title Only Author and Title](#)

Sims DA, Gamon JA (2003). Estimation of vegetation water content and photosynthetic tissue area from spectral reflectance: a comparison of indices based on liquid water and chlorophyll absorption features. Remote Sensing of Environment 84: 526–537.

Pubmed: [Author and Title](#)
Google Scholar: [Author Only Title Only Author and Title](#)

Song Y, Yang C, Gao S, Zhang W, Li L, Kuai B. (2014). Age-triggered and dark-induced leaf senescence requires the bHLH transcription factors PIF3,4, and 5. Molecular Plant 7: 1776-1787.

Pubmed: [Author and Title](#)
Google Scholar: [Author Only Title Only Author and Title](#)

Spicher L, Almeida J, Gutbrod K, Pipitone R, Dörmann P, Glauser G, Rossi M, Kessler F. (2017). Essential role for phyto kinase and tocopherol in tolerance to combined light and temperature stress in tomato. Journal of Experimental Botany 68: 5845–5856.

Pubmed: [Author and Title](#)
Google Scholar: [Author Only Title Only Author and Title](#)

Spicher L, Glauser G, Kessler F. (2016). Lipid Antioxidant and Galactolipid Remodeling under Temperature Stress in Tomato Plants. Frontiers in Plant Science 7: 167.

Pubmed: [Author and Title](#)
Google Scholar: [Author Only Title Only Author and Title](#)

Stephenson PG, Fankhauser C, Terry MJ. (2009). PIF3 is a repressor of chloroplast development. Proceedings of the National Academy of Sciences 106: 7654–7659.

Pubmed: [Author and Title](#)
Google Scholar: [Author Only Title Only Author and Title](#)

Suwa R, Hakata H, Hara H, El-Shemy HA, Adu-Gyamfi JJ, Nguyen NT, Kanai S, Lightfoot DA, Mohapatra PK, Fujita K. (2010). High temperature effects on photosynthate partitioning and sugar metabolism during ear expansion in maize (Zea mays L.) genotypes. Plant Physiology and Biochemistry 48: 124–130.

Pubmed: [Author and Title](#)
Google Scholar: [Author Only Title Only Author and Title](#)

Takahashi S, Murata N. (2008). How do environmental stresses accelerate photoinhibition? Trends in Plant Science 13: 178–182.

Pubmed: [Author and Title](#)
Google Scholar: [Author Only Title Only Author and Title](#)

Toledo-Ortiz G, Johansson H, Lee KP, Bou-torrent J, Stewart K, Steel G, Rodríguez-Concepción M, Halliday KJ. (2014). The HY5-PIF Regulatory Module Coordinates Light and Temperature Control of Photosynthetic Gene Transcription. PLoS Genetics 10: 10.1371/journal.pgen.1004416.

Pubmed: [Author and Title](#)
Google Scholar: [Author Only Title Only Author and Title](#)

Tomato Genome Consortium. (2012). The tomato genome sequence provides insights into fleshy fruit evolution. Nature 485: 635–641.

Pubmed: [Author and Title](#)
Google Scholar: [Author Only Title Only Author and Title](#)

Van Eerden FJ, De Jong DH, De Vries AH, Wassenaar TA, Marrink SJ. (2015). Characterization of thylakoid lipid membranes from cyanobacteria and higher plants by molecular dynamics simulations. Biochimica et Biophysica Acta - Biomembranes 1848: 1319–1330.

Pubmed: [Author and Title](#)
Google Scholar: [Author Only Title Only Author and Title](#)

Velikova V, Varkonyi Z, Szabo M, Maslenskova L, Nogues I, Kóvacs L, Peeva V, Busheva M, Garab G, Sharkey TD, Loreto F. (2011). Increased Thermostability of Thylakoid Membranes in Isoprene-Emitting Leaves Probed with Three Biophysical Techniques. Plant Physiology 157: 905–916.

Pubmed: [Author and Title](#)
Google Scholar: [Author Only Title Only Author and Title](#)

Watson ML. (1958). Staining of Tissue Sections for Electron Microscopy with Heavy Metals: II. Application of Solutions Containing Lead and Barium. The Journal of Cell Biology 25: 727–730.

Pubmed: [Author and Title](#)
Google Scholar: [Author Only Title Only Author and Title](#)

Wellburn A (1994). The spectral determination of chlorophylls a and b, as well as total carotenoids, using various solvents with spectrophotometers of different resolution. Journal of Plant Physiology 144: 307-313.

Pubmed: [Author and Title](#)
Google Scholar: [Author Only Title Only Author and Title](#)

Weller JL, Schreuder MEL, Smith H, Koornneef M, Kendrick RE. (2006). Physiological interactions of phytochromes A, B1 and B2 in the

control of development in tomato. *Plant Journal* 24: 345–356.

Pubmed: [Author and Title](#)

Google Scholar: [Author Only](#) [Title Only](#) [Author and Title](#)

Yamori W, von Caemmerer S. (2009). Effect of Rubisco Activase Deficiency on the Temperature Response of CO₂ Assimilation Rate and Rubisco Activation State: Insights from Transgenic Tobacco with Reduced Amounts of Rubisco Activase. *Plant Physiology* 151: 2073–2082.

Pubmed: [Author and Title](#)

Google Scholar: [Author Only](#) [Title Only](#) [Author and Title](#)

Yuan XY, Wang RH, Zhao XD, Luo YB, Fu DQ. (2016). Role of the tomato Non-Ripening mutation in regulating fruit quality elucidated using iTRAQ protein profile analysis. *PLoS ONE* 11: 10.1371/journal.pone.0164335.

Pubmed: [Author and Title](#)

Google Scholar: [Author Only](#) [Title Only](#) [Author and Title](#)

Zhang Y, Liu Z, Chen Y, He, J, Bi Y. (2015). PHYTOCHROME-INTERACTING FACTOR 5 (PIF5) positively regulates dark-induced senescence and chlorophyll degradation in Arabidopsis. *Plant Science* 237: 57-68.

Pubmed: [Author and Title](#)

Google Scholar: [Author Only](#) [Title Only](#) [Author and Title](#)

Zhang Y, Mayba O, Pfeiffer A, Shi H, Tepperman JM, Speed TP, Quail PH. (2013). A Quartet of PIF bHLH Factors Provides a Transcriptionally Centered Signaling Hub That Regulates Seedling Morphogenesis through Differential Expression-Patterning of Shared Target Genes in Arabidopsis. *PLoS Genetics* 9: 10.1371/journal.pgen.1003244.

Pubmed: [Author and Title](#)

Google Scholar: [Author Only](#) [Title Only](#) [Author and Title](#)

Zhang R, Sharkey TD. (2009). Photosynthetic electron transport and proton flux under moderate heat stress. *Photosynthesis Research* 100: 29-43.

Pubmed: [Author and Title](#)

Google Scholar: [Author Only](#) [Title Only](#) [Author and Title](#)

Zhao C, Liu B, Piao S, Wang X, Lobell DB, Huang Y, Huang M, Yao Y, Bassu S, Ciais P, Durand JL, Elliott J, Ewert F, Janssens IA, Li T, Lin E, Liu Q, Martre P, Müller C, Peng S, Peñuelas J, Ruane AC, Wallach D, Wang T, Wu D, Liu Z, Zhu Y, Zhu Z, Asseng S. (2017). Temperature increase reduces global yields of major crops in four independent estimates. *Proceedings of the National Academy of Sciences* 114: 9326–9331.

Pubmed: [Author and Title](#)

Google Scholar: [Author Only](#) [Title Only](#) [Author and Title](#)

Zhao F, Zhang D, Zhao Y, Wang W, Yang H, Tai F, Li C, Hu X. (2016). The Difference of Physiological and Proteomic Changes in Maize Leaves Adaptation to Drought, Heat, and Combined Both Stresses. *Frontiers in Plant Science* 7: 1471.

Pubmed: [Author and Title](#)

Google Scholar: [Author Only](#) [Title Only](#) [Author and Title](#)

Zhou Y, Xun Q, Zhang D, Lv M, Ou Y, Li J. (2019). TCP Transcription Factors Associate with PHYTOCHROME INTERACTING FACTOR 4 and CRYPTOCHROME 1 to Regulate Thermomorphogenesis in Arabidopsis thaliana. *iScience* 15: 600-610.

Pubmed: [Author and Title](#)

Google Scholar: [Author Only](#) [Title Only](#) [Author and Title](#)

Competing interests

The authors declare no competing interests.